Structural and Optical Properties of Gold Nanoparticle Embedded Solution Processed Zinc Oxide Thin Films

A thesis submitted in partial fulfilment of requirement for

the award of degree in

Masters of Science

in

Physics

Submitted By

Sargun Kaur

Regd. No. 301504032

Under the guidance of

Dr. Bhaskar Chandra Mohanty

Associate Professor

School of Physics and Materials Science

Thapar University

(Established under section 3 of UGC Act, 1956)

Patiala-147001, India

July 2017

Dedicated

To

My Parents

CERTIFICATE

This is to certify that the report entitled ***"Structural and Optical Properties of Gold Nanoparticle Embedded Solution Processed Zinc Oxide Thin Films"*** submitted by **Sargun Kaur, Roll No. 301504032**, student of M.Sc. Physics, Thapar University, Patiala, was carried out by her under my supervision. She has not submitted this material for the credit towards any other degree at Thapar University, Patiala or at any other university.

Dr. Bhaskar Chandra Mohanty

Associate Professor

School of Physics and Materials Science

Thapar University, Patiala

ACKNOWLEDGEMENT

In pursuit of this academic endeavour, I feel that I have been especially fortunate as inspiration, guidance, direction, co-operation, love and care all came in my way in abundance and it seems almost an impossible task for me to acknowledge the same in adequate terms.

I express my sincere thanks to my supervisor, to **Dr. Bhaskar Chandra Mohanty**, Designation, School of Physics and Materials Science, Thapar University, Patiala, for his esteemed supervision, incessant support, inspiration and constructive criticism throughout my research work.

I accord my thanks to **Dr. Manoj K. Sharma**, Professor and Head, School of Physics and Materials Science, Thapar University, Patiala, for providing me with the opportunity to conduct this work and bring it out in the present form.

I offer special thanks and regards to **Ms. Indu Gupta, Mr. Kaushlendra Pandey, Ms. Chhavi Pahwa** for providing me immense support in performing characterizing and evaluating this thesis work.

I would also like to thank my friends Ishjot Singh, Ravikiran Kaur, Arshjot Kaur for helping me throughout the degree.

Finally, I would like to express my sincere gratitude to my parents, for their encouragement and moral support, which always inspired me and stood by me as strong pillars.

Sargun Kaur

Regd. No. 301504032

ABSTRACT

This thesis deals with the growth and characterisation of gold nanoparticle embedded ZnO thin films. ZnO thin films were synthesised by solution process using reagents like zinc acetate dihydrate, 2-methoxyethanol and monoethanolamine. Parameters like ageing period, annealing duration and number of layers were changed to optimise the growth. Gold nanoparticles were prepared by the direct current sputtering route. Amount of gold was changed to observe its effect on the films. The properties of the so formed films was checked by Thermogavimetric analysis/Differential Scanning Calorimetry (TGA/DSC), X-ray Diffraction (XRD), UV-Vis spectroscopy and Scanning Electron Microscopy (SEM) characterisation. The formation of the ZnO solution is studied from TGA/DSC analysis. It gave decomposition peaks and boiling points of all the reagents and the solution. Detailed structural analysis was carried out by the XRD measurements. The XRD patterns exhibited peaks from various planes of wurtzite ZnO and FCC Au. The SEM studies showed a change in surface ,morphology of the films when Au particles were introduced in the sandwich structure. Optical features were tested by UV-Vis spectroscopy. It showed clear absorption peaks due to the surface plasmon resonance (SPR) of Au nanoparticles suggesting that annealing led to the dewetting and agglomeration of the Au layer. The SPR peak position shifted depending on the annealing duration showing tuning of the optical properties of the sandwich structure.

LIST OF FIGURES

Figure	Title	Page No.
1.1	Crystal structure of ZnO	4
2.1	Pictorial view of spin coating machine	14
2.2	Outlook of DC sputtering machine	15
2.3	Schematic of growth of solution required for Spin coating process	17
2.4	Flowchart of the solution process and the spin coating method employed	18
2.5	Schematic of working criteria of spin coating method	18
2.6	Schematic of DC sputtering machine	19
2.7	Glances of the sample with bottom layer of ZnO and above layer of Au	20
2.8	Final samples with triple layered films	21
2.9	Pictorial presentation of film so formed	21
2.10	Schematic of internal working of TGA	22
2.11	Schematic of internal working of DSC measurement	23
2.12	TGA/DCS Equipment	23
2.13	Principle of Bragg's Law	25
2.14	Showing overall idea of working of XRD and XRD system itself	25
2.15	Schematic of internal working of UV-VIS Spectrometer	26
2.16	Outlook of the UV-VIS Spectrometer	27
2.17	Schematic of internal working of SEM system	28
2.18	Picture of SEM instrument	29
3.1	Showing typical TGA/DSC curves of the chemicals used for preparing the ZnO thin films via spin coating technique	30
3.2	XRD patterns showing effect of aging on virgin and Annealed sample of ZnO thin films	32
3.3	Illustrating effect of annealing duration on samples coated with (a) 15 layers, (b) 30 layers and (c) 50 layers.	33

3.4 Depicting the effect of concentration of Au in sandwich structure when Au was annealed for different periods as in (a) 6hrs, (b) 4hrs. 33

3.5 Exhibiting effect of concentration of Au in as deposited ZnO/Au film by deposition Au via sputtering method for 0, 1, 2, 3min. 35

3.6 Presenting the effect of annealing duration on Au in ZnO/Au when latter layer is sputtered for (a) 1min, (b) 2min, (c) 3min. 35

3.7 Showing the effect of varying concentration of gold in ZnO/Au and ZnO/Au/ZnO films 37

3.8 Exhibiting the effect of annealing period and concentration of Au in Sandwich structure 37

3.9 SEM images of various SEM samples at two distinct magnification 1μm and 5μm 39

CONTENTS

CERTIFICATE	**iii**
ACKNOWLEDGEMENT	**iv**
ABSTRACT	**v**
LIST OF FIGURES	**vi**
CHAPTER 1 INTRODUCTION	**1**
1.1 Thin Films	1
1.2 ZnO	3
1.2.1 Structure	3
1.2.2 Properties	4
1.3 Nanoparticles embedded ZnO	5
1.4 Uses	5
1.5 Literature Review	6
1.6 Motivation and Objective	12
CHAPTER 2 EXPERIMENTAL DETAILS	**13**
2.1 Growth of ZnO-Au thin films	13
2.1.1 Deposition Technique for ZnO thin films	14
2.1.2 Coating Technique for Gold Nanoparticles	15
2.2 Mechanism	16
2.3 Characterisation Techniques	21
2.3.1 TGA/DSC	21
2.3.2 X-Ray Diffraction (XRD)	23
2.3.3 UV Spectroscopy	26
2.3.4 SEM	27
CHAPTER 3 EXPERIMENTAL RESULTS AND DISCUSSION	**30**
3.1 TGA/DSC Studies	30
3.2 XRD Studies	31
3.3 UV-Vis Spectroscopy Analysis	34
3.4 SEM Analysis	38
CHAPTER 4 CONCLUSIONS	**42**
REFERENCES	**44**

CHAPTER 1

INTRODUCTION

1.1 Thin films

Thin films are two dimensional structures with thickness ranging from few micrometers to nanometers. The thin films find applications in areas such as LEDs, LCDs, optical coatings (such as antireflective coatings) [1,2], electronic semiconductor devices, pharmaceuticals (as in thin film drug delivery) [3], hard coatings on cutting tools, magnetic recording media, micro-mechanics, and both for energy generation (e.g. thin film solar cells) and storage (e.g. thin film batteries) etc. The main motive of imbibing thin films is weight reduction and bulkiness of the materials by reducing the amount of material used. They fulfill the requirements needed for the application and also offer low cost processing.

In addition to their applications required, thin films also play a crucial part in the development of materials and their study with fresh and exclusive (exceptional) properties. Ability to selectively and controllably deposit thin films guarantees progress in each areas. Often control is required, even at the atomic level of film microstructure and microchemistry. Even for high priced or costly raw source materials, cost effective applications could be made possible. Latest developments and researches in optoelectronic device applications make it important that improvisations must be made in physical and chemical properties of conducting oxide films.

The importance of thin films has and remains to be significant and have been continuously used for improving the surface properties of solids. Many properties of a bulk material surface are/could be improved with the help of a thin film. Examples are transmission, absorption, reflection, hardness, abrasion resistance, corrosion, permeation, electrical behavior etc. Also, the basis of Nanotechnology is derived from thin film technology.

The categorization of thin films is done in many ways, mainly, in accordance to materials needed for the coatings, strength, damage threshold and characteristics etc. For instance, the metallic coatings have a good level of absorption and only limited applications but on the other hand, dielectric coatings have insignificant absorption level and therefore, they are handy for other optic applications e.g. laser systems as well as imaging instruments.

Thin films have numerous applications for a large variety of industrial work. For instance, corrosion and wear-tear resistant coatings, which are able to extend the life of a great number of vital products. Also, optically and electrically active as well as magnetic thin films can be employed in solar cells, thin film electro acoustic devices, sensors, actuators, porous nanocomposite films etc [4].

The technology of thin films finds its applications for tailoring coating materials for particular purposes. This technology for tribological applications can also be used for producing super hard and tough coatings, and also self lubricating coatings. Smart windows of electrocromic controlled transparency have been inspected. Efforts on magnetic properties of thin films which include synthesis of piezoelectric and ferroelectric thin films are being put and reported.

To optimize the surface properties, coatings are being used now-a-days on tools for metal cutting and also forming and on the machine elements, like bearings, seals gears, and valves.

Recently there have been extensive studies on transparent conducting oxide (TCO) thin films. They have evolved as an important group of materials owing to their properties and critical to many applications. For example, transparent electrodes are required for electro-optical devices and for that solar cells and flat panel displays are quite significant examples.

For both the electrodes of Liquid Crystal Displays (LCDs), TCO films are required, as while applying voltage to the various pixels, there is necessity for backlighting to transmit through the liquid crystal film [5].

For a number of years now, thin film technology has been a main topic in solar cell research. Lately, new as well as less expensive thin film based solar cells have reached the competance of crystalline silicon solar cells. TCO films are being used in most solar cells as a transparent electrode. Other than conductivity and transparency, other factors of TCO for this purpose are electronic compatibility with adjoining layers in the cell, processing requirements and stability under environmental conditions. Mostly, films chosen for such an application are tin oxide based films because patterning is not the requirement but environmental stability is essential.

The architectural use of TCOs is majorly for energy efficient windows. Because of their lower thermal emittance compared to uncoated glass, tin oxide (a TCO) coated windows are capable of preventing radiative heat loss and thus are perfect to utilize in cold or moderate climate.

TCO coatings are used to construct transparent heating elements. These are useful as vehicular windshields and defrosters in aircraft. Their benefit over conventional hot air

blowers is that they work uniformly over large area and can have a much shorter effective defrosting time.

In order to reduce electromagnetic radiation interference TCO coatings may be used as shielding while giving visual access. This may be used to avoid either from entering an enclosure to prevent external radiation sources from interfering with electronic devices within or to keep radiation from escaping an enclosure to prevent interfering with nearby devices / detection.

Daily use example is the window of domestic microwave ovens. To reduce microwave leakage, we employ aperforated metal screen today [which hinders clear visual observation].

1.2 ZnO

ZnO is treated as a material of gigantic technological importance because of its properties. It finds applications in optoelectronic devices for instance Light emitting diodes (LED), Solar cell, Optical wave guide, Biosensors, Transparent thin film transistor, Photocatalyst and Surface acoustic wave (SAW) devices. Because of the fascinating properties as well as applications of ZnO, attention is being given to its study in thin film form [6].

1.2.1 Structure

Most of the group II-VI binary compound semiconductors crystallize in either hexagonal wurtzite or cubic zinc–blende structure as illustrated in **Figure 1.1** where four cations surround each anion at the corners of the tetrahedron and vice versa**.** Its rocksalt structure is only observed at relatively high pressure of around 10GPa. ZnO is found as white powder which is known as the mineral zincite or as zinc white also. The crystallization of ZnO happens in the wurtzite lattice.

Zinc atoms are almost in the position corresponding to the structure of hexagonal close packed (hcp) lattice. Every oxygen atom lies within the four zinc atoms forming tetrahedral group. For the polar symmetry, this crystal has all these tetrahedral points in the same direction along the hexagonal axis. a= 3.24 Å and c= 5.19 Å ate the lattice constants [7].

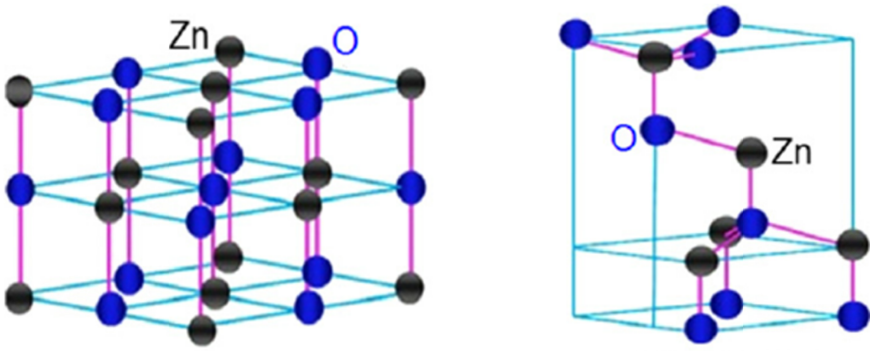

Figure 1.1: Crystal structure of ZnO.

1.2.2 Properties

1. The ZnO based films consist of cheap and abundant elements, where as the In containing films are more expensive.
2. They are nontoxic and is obtained as white powder.
3. It has a very high melting point of 2248K.
4. They can be produced by the sol–gel process easily, it is being preferred for large-scale architectural coatings.
5. They allow customising the UV absorption, which seems expected since the fundamental bandgap of ZnO lies just at the end of the luminous spectrum at 3.37 eV [8].
6. The utmost important feature in case of amorphous and microcrystalline silicon related fields is to show stability in hydrogen plasma but the problem occurs in case of tin oxide (SnO_2) and indium oxide (In_2O_3) as when they are exposed to hydrogen plasma, they get reduced to metallic forms.
7. It is n-type semiconductor with a high breakdown voltages, high melting temperature and also ability to sustain large electric field, high-temperature, lower noise generation, and high-power operation. It has large exciton binding energy of about 60 meV.

It is particularly attractive as films have good quality with Hall mobilities and can be made at room temperature. As a result, there is a decent compatibility with flexible or plastic substrate materials. Since a ZnO semiconductor is transparent in the visible region and are therefore less light sensitive. TFTs based on ZnO may have particular advantage in solar cells with high efficiency and in electronic drivers for displays. ZnO is also a suitable material for phosphor applications due to its strong luminescence in the green–white region of the spectrum [9,10].

1.3 Au Nanoparticles embedded ZnO thin films

In recent years, many research groups have studied metal nanoparticle embedded ZnO thin films. These films yield quite unusual properties and have found applications in many emerging research areas [11-15].

The addition of flexibility or development of new applications are brought about to existing systems in many areas like microelectronics, catalysis, optics etc. by introducing the size-induced properties of nanoparticles (NPs). Particularly, nanoparticles of noble metals such as gold (Au) and silver (Ag) have been gaining more attention than platinum (Pt) or Copper (Cu) or Palladium (Pd), because they display a range of colours in the visible region based on the surface plasmon resonance. This property is a consequence of the collective oscillations of the electrons at the surface of the nanoparticles. The exclusive features of the plasmon absorption in these noble metal NPs have been exploited for a wide range of applications. Optical properties of noble metal nanoparticles in various solid matrices have been studied widely.

ZnO is an apt option for optical applications due to its low reflection and high transparency within the visible – IR spectral range. It represents an ideal raw material for the growth of the Au NPs to investigate their optical characteristics due to absence of role of ZnO in the absorption or reflection spectra in the visible-IR spectral range.

Hence, out of several inert metals, Au is chosen as it enhances optical and electronic properties of hybrid like high electrical conductivity, has exceptional thermal stability that most metals do not have, has the ability to resist corrosion and also ZnO provides a good electron transport path for electrons emitted from Au NPs [16].

1.4 Uses

Lately, new possibilities and opportunities of synthesizing engineered materials with enhanced electrical, optical, and surface properties are opening because of deposition of noble metal nanoparticles on surface of metal oxide semiconductors.

Semiconductors, viz. TiO_2 and ZnO with wide bandgap absorb mainly the UV light. If we combine these materials with metal nanoparticles, viz. silver, gold and platinum, this may shift their absorption threshold to visible region from UV region. Also, we can alter to other semiconductor properties.

Nanocomposite (NCs) films that has metal particles in the scale of a few to several nanometers (nm) embedded in metal oxides have proved to be useful applications in catalysis, photocatalysis, sensors and novel optoelectronic devices owing to their various useful optical and electronic properties as a result of quantum size effects [17,18].

In order to improve photo catalytic activity by locking in the photo induced charge carriers as well as boosting the charge transfer processes, a blend of semiconductor substrate (i.e. ZnO and TiO_2) and noble metal cluster (such as Ag, Pd, Au and Pt) is observed. The noble metals of Au and Pt were employed for the metal- ZnO formation, the reason being their high electron affinity behaviour. The most inert metallic element is Au with attractive properties as a heterogeneous catalyst [19].

Application of the enhancement of the devices such as photo detectors, gas sensors, light emitting diodes, solar cell have already been seen.

1.5 Literature Review

The literature has been reviewed in detail to get the full insight of the research work.

(1) Patra *et al.* [20] studied that ZnO film showed more than 80% transmittance in visible region and, single and double layers of gold nanoparticles showed transmittance around 600nm, reducing the transmittance by 25%. This was when ZnO films were prepared by pulsed magnetron sputtering and sandwiching Au nanoparticles were embedded by thermal evaporation. Localised surface plasmon resonance (LSPR) peak was red shifted to 615nm from 558nm when covered with ZnO film. Gold nanoparticles embedded sandwiched structure showed great reduction in UV photoluminescence which was major in pure ZnO films. This was creditted to the interband absorption in Au. Thus multilayered structures of gold nanoparticles embedded in ZnO thin films may be good aspirant for UV absorbers and red/yellow optical filters.

(2) Huang *et al.* [21] investigated the effect of embedded gold nanoparticles on electrical properties of ZnO in order to have a highly conductive oxide semiconductor. ZnO layer was prepared by spin coating and the mid gold layer was coated by e-beam evaporation. Gold NPs affected both electrical and structural properties of the resultant films. There were electron emissions to the ZnO matrix from gold NPs. This was the cause of decrease in electrical resistivity by five orders of magnitude.

Electron mobility in the film is limited by Au/ZnO heterogenous interface at higher temperature and grain boundary at lower temperature. At the lower temperature, NPs of Au donate electrons by tunneling to ZnO matrix. Else they are thermally emitted across schottky barrier at the interface of both the layers. Embedded gold NPs alter microstructure of ZnO matrix and improves electron mobility. Depending on amount of gold, transmittance spectra ranged from 68% to 85%. As the thickness of Au increased, transmittance decreased wherein double layer of ZnO with no gold layer shows 93% transmittance.

(3) Shan *et al.* [22] prepared ZnO/Au nanocomposites via solution routes and formed heterostructured nanoparticles through epitaxial growth of Au on ZnO seeds. The nanocontact between the two films resulted in red shift of the surface Plasmon peak of Au and also increased intensity of Raman signals of ZnO. Reason for latter is that there is interfacial charge transfer between metal gold and ZnO nanocrystals. Point defects on ZnO surface trap gold atoms and help in crystal growth. This heterostructured nanocomposite so obtained, in addition, enhanced chemical stability of Zn in aqueous solution.

(4) Mehrani *et al.* [23] looked into optical properties and structural change of Au/ZnO. Preparation of Au/ZnO nanocomposites was by laser irradiation of mixed colloidal suspension. Properties were studied as a function of volumetric ratio of ZnO and Au colloidal suspension in water. The results of XRD depicted polycrystalline Au structure. UV-vis analysis revealed plasmon peak of the nanocomposite was broadened and red shifted in comparison to pure gold NPs. Band gap energy was calculated 3.15eV-3.27eV for this nanocomposite. Room temperature PL spectrum showed that with increased conc. of Au, intensity increased of the visible emission band. TEM images of these nanocomposites showed increasing adhesion with increase in volumetric ratio of Au colloidal suspension.

(5) Gaspera *et al.* [24] examined electrical gas sensing response and enhanced optical properties of ZnO/Au nanostructured thin films and also of NiO/Au films. Both the films were grown by sol gel process. XRD results revealed that films were crystalline.They showed optical absorption in the visible range is in accordance to gold NPs concentration in UV-Vis analysis. Gold NPs have proved to improve optical

sensing properties over surface Plasmon resonance resonance (SPR) peak wavelength range for both NiO and ZnO, and near UV range for ZnO where gold is optically inactive. Gold showed an enhancing effect in sensing performances in electrical response as combining shift in SPR peak and different semiconductive types of oxides. Au detected charge variation and injection of electron by reducing gases into oxides by its catalytic activity.

(6) Balevicius *et al.*[25] explored influence of localised plasmons of the Au/ZnO nanostructure on the optical properties. ZnO layer was prepared by atomic layer deposition and Au by physical vapour deposition. With increase in thickness of Au, transition from cluster to thin films is revealed from structural and optical parameters. Optical analysis showed that there was little change in localised Plasmon peaks in absorption spectra. These changes make prominent contribution to refractive index of Au film. Further resulting in significant enhancement of UV photoluminescene peak in ZnO. Due to changes in structure properties of Au layer, optical dispersion can be tuned of each layer and thus control enhancement of PL spectra of ZnO. And quench is possible in UV- visible region.

(7) Dixit *et al.* [26] researched optoelectronic property of ZnO thin films with the help of Au. Former was prepared via solution route-spin coating and the latter by sputtering. Compared to ZnO films, enhancement was seen in UV and visible light emission in ZnO/Au and ZnO/Au/ZnO whereas quenching was observed for Au/ZnO in PL spectrum. Excitation intensity dependent PL spectrum inflicted dominance of horizontal dipole surface plasmon mode for ZnO/Au and ZnO/Au/ZnO, which led to enhanced orange and greenish yellow emission respectively. Absorption was selectively enhanced in UV visible region by varying configuration of ZnO and Au. This attribute can be assigned to interaction of dipole SPR with photon subsystem and localised trapping levels. Au layer being sandwiched or being on top or being at bottom have different results. Metal layer at the bottom and in middle of sandwich structure is suited for enhanced UV- visible emission, while metal coated on top of ZnO films is suited for passivation of emissions related to defects. Also, UV absorption was enhanced selectively for semi-conductor/metal while semiconductor/metal/semiconductor showed visible region enhancement.

(8) Liu *et al.* [27] fabricated Au/ZnO nanostructure with smaller ZnO NPs stacked onto bigger Au NPs through sol-gel method and combining seed mediated method. This stacking causes change in environment surrounding Au leading to change in dielectric constant. The obtained Au/ZnO showed properties in photocatalysis process like methyl orange (MO) degradation etc. These improved properties were due to the SPR effect of gold NPs, which could chip in to the parting of photo-excited holes and electrons and assist the process of absorption of visible light. The work contributes to the emerging multi-functional nanocomposites with uses in visible light driven photocatalysts and makes the choice Au/ZnO photocatalyst unusual.

(9) Chen *et al.* [28] inspected 3D flower-like Au-ZnO microstructures synthesized by a facile one-step aq. solution route at room temperature resulting in controlled morphology and dimensions. Photocatalytic properties were studied. Investigation of growth process of Au-ZnO and the consequence of trisodium citrate on growth and nucleation of ZnO was observed. Pure ZnO had lower photocatalytic activity than that of Au-ZnO structures. Better photocatalytic activity of Au-ZnO was credited to strong electronic interaction between ZnO and Au NPs.

(10) Kumari *et al.* [29] inspected nanostructured ZnO thin films loaded with silver/gold nano-isles. Former prepared by sol gel method and latter by electrodeposition. Deposition of nano-isles induced surface heterogeneity into the resultant films. XRD indicated formation of wurtzite ZnO phase, with diffusion of gold/silver into zinc oxide lattice. Though changes in the bandgap were not significant. Samples showed gain in photoelectrochemical (PEC) water splitting current, which is characteristic to role played by transport of photogenerated charge-carriers and gold/silver nano-isles in the separation.

(11) Garcia-Serrano *et al.* [30] scrutinized making Metal (Au, Cu, Pt)/zinc oxide nanocomposite (NCs) films by radio frequency (RF) co-sputtering technique to study structural and optical properties. TEM showed that with increase in annealing temperature, size of particles of noble metal also varied in matrix of ZnO. SPR bands were seen in the Cu doped ZnO and Au doped ZnO composite films because of the formation of nm-size Cu and Au particles. it shows dependence on annealing temperature and content of metal. However, a Pt/ZnO composites didn't show similar

behaviour. The optical bandgap of the matrix was reduced drastically, on merging Pt NPs in the ZnO matrix.

(12) Stavale *et al.* [31] analyzed ZnO thin film grown on a Au(111). Lattice mismatch with the metal (Au) beneath causes ZnO to give ordered hexagonal pattern with (0001)-orientation. This superstructure disappears at low thickness of film. Conductance spectroscopy and STM-based luminescence shows that the ZnO bandgap reaches the bulk value in thicker films. Photon peaks with sub-band-gap energies tells that defects existing in the wurzite lattice. An adsorption-mediated compensation system seen in thick films and in thin ones, the intrinsic polarity of the ZnO (0001) surface is explained by reduction in distance of Zn−O interlayer.

(13) Chamorro *et al.* [32] considered gold nanoparticles embedded in zinc oxide (ZnO-Au) NCs films to study photoluminescence enhanced by local structure driven LSPR. The films synthesized with different Au concentration by reactive magnetron sputtering and annealing in air up to 300 °C. During deposition, gold substitutes zinc as isolated atoms and as nanoparticles in ZnO lattice and still exhibited the ZnO structure. Both degraded the crystalline quality of the ZnO matrix, but annealing helped it cure from isolated Au atoms and triggers the formation of Au NPs of size higher than 3 nm, which is sufficient to observe localized surface plasmon resonance (LSPR) peak. The amplitude of absorption peak after annealing increases with the Au loading and temperature. Even, UV and visible PL from the ZnO matrix is enhanced by activation of LSPR indicating great coupling with the Au NPs. Spectroscopic ellipsometry measurements depicted how curing the defects modified the optical dielectric functions of the nanocomposite and ZnO matrix and increased the bandgap of ZnO matrix.

(14) Liao *et al.* [33] probed Au:oxide composite multilayer films prepared by magnetron sputtering consisting of Au nanoparticles sandwiched by oxide layers such as SiO_2, ZnO, and TiO_2. Photoluminescene peaks located at a wavelength between 590 and 680 nm were observed, with Au particle size varying from several to hundreds of nanometers. It was noticed that the surface plasmon resonance (SPR) in these exerted little effect on the PL intensity but a strong affect on the position of the PL peaks.

(15) Tarwal *et al.* [34] scrutinized the ZnO-Au thin films prepared by spray pyrolysis technique. Absorption bands induced via surface Plasmon resonance (SPR) in the visible region have been observed. The evolution of the SPR absorption with Gold incorporated concentration is shown. The optical studies were carried out at room temperature by using spectrofluorometer and UV-Vis Spectrophotometer. It showed a broad LSPR absorption band, which red shifted and became narrower with an increase in amount of Au. XRD study reveals that the Au concentration increases, the Au showed gradual evolution with sharpening of the peak. Whereas the ZnO planes began to improve after doping of Au. These thin films were used for photoelectrochemical (PEC) application as, in dark, rectifying behaviour showed in I-V and curves are shifted to the fourth quadrant under illumination, suggesting that the samples are generator of electricity.

(16) Ozga *et al.*[35] deposited Au NPs on ZnO nanocrystalline films to explore photoinduced second harmonic generation (SHG). They established coexistence of ZnO and Au NPs gave larger SHG as compared to pure ZnO nanocrystalline. Nonlinear optical susceptibilities obtained during phototreatment were better around 30-35^{o}C for samples doped with Au. Decrease in optical SHG is seen with increasing temperature. Samples without Au are independent of temperature.

(17) Lee *et al.* [36] prepared Au interlayer ZnO films by radio frequency and direct current sputtering. Effect of annealing was examined on structural, optical and electrical properties of the resultant film. XRD peak intensities seemed to increase after annealing. As deposited films showed low resistivity and after annealing it decreased even further from 2 X 10^{-4} to 9.8 X $10^{-4}\Omega$ cm. Also with increase in annealing temperature, work function of the films also increase as 300^{o}C annealed has higher work function of 4.1eV than the one annealed at 150^{o}C.

1.6 Motivation and Objective

The brief literature review presented above shows the huge application potential of the Au NP embedded in ZnO thin films and form the basis of this work. While a variety of cases are reported for making the ZnO thin films, spin coating technique has been recognized as a promising one due to easy process steps and cost competitiveness. Au nanoparticles can be

grown by a modified sputtering technique. We have used these techniques to prepare the Au NP embedded ZnO films and investigated their structural and optical properties in detail.

The objectives of this work are:

(i) to prepare Au NP embedded ZnO thin films.

(ii) to study structural and optical properties of these films as a function of heat treatment given to the Au layer and the Au concentration.

CHAPTER 2

EXPERIMENTAL DETAILS

This chapter deals with the growth of the Au NPs embedded ZnO thin films and detailed characterisation thereof. The ZnO films were grown by the technique of spin coating and the Au NPs were embedded by the DC sputtering technique.

2.1 Growth of ZnO and Au thin films

Thin films are known to be prepared by a variety of techniques, such as RF magnetron sputtering, reactive magnetron sputtering, ion-beam evaporation, electron-beam evaporation, chemical vapor deposition, vacuum arc deposition, spray pyrolysis, laser ablation etc [37]. All processes have their specific limitations and involve compromises with respect to method specifics. Among all the various techniques available, the spin coating method seems to be the most attractive. It is simple, economical, and environmentally friendly and offers a method for a large-scale deposition of ZnO thin film at low cost, but also opens a way to the size-controlled fabrication of other materials, also we get coating on the desired area and of desired shape, it is easy control of the concentration of the solution, doping level, and homogeneity without the use expensive equipment [38-43].

Disadvantage is that the sheet resistance of the films produced by this method is usually at least one order of magnitude higher than that of the sputter-coated films. Other possible reason is that there are many more parameters which need to be optimized in sol-gel processes. Choice of precursors, number of layers deposited, drying temperature, annealing temperature and atmosphere all could play a crucial role in shaping the properties of the deposited thin films. Also, as sol-gel procedures are much more manual, good quality films are less reproducible than sputter-coated ones. However, by going through careful optimization and process control, this technique shows enormous potential in becoming the preferred low cost deposition method of the future.

2.1.1 Deposition technique for ZnO thin films

The sol-gel process is a low-temperature process that uses inorganic or metal organic precursors to produce metal oxide molecules in solution form. The solution is synthesised based on the condensation and hydrolysis reactions of organometallic compounds in alcohol-based solutions. Several methods can then be used to deposit ZnO films using the solutions, our concern is with Spin-Coating (instrument in **Figure 2.1**). For this technique, the material to be deposited is dissolved or dispersed into a solvent, and this solution is then coated onto the substrate surface and spun off to have a uniform layer of thin film on the substrate.

The four key phases in the spin-coating process are:

1. Deposition of solution onto the substrate.

2. Spreading of solution from centre of substrate to the sides (spin-up).

3. Gradual thinning of solution (spin-off).

4. Gelation due to solvent evaporation.

As the fabricated film is thinned by the centrifugal draining, it tends to be uniform since centrifugal force acting outwards forms a balance with the radially viscous force that acts inwards. Even with non-planar substrates, very homogeneous film thicknesses can be achieved [44].

Figure 2.1: Outlook of spin coating machine.

2.1.2 Coating technique for Gold Nanoparticles

Direct Current (DC) Sputtering is in disguise a Thin Film Physical Vapor Deposition (PVD) Coating technique. It is used extensively in the semiconductor industry creating microchip circuitry on the molecular level. It involves use of a target material as the coating material is bombarded with ionized molecules of gas causing atoms to be Sputtered off into the plasma. These vaporized atoms are then deposited on the substrate opposite to the target, it is then that they condense as a thin film to be coated.

DC Sputtering is the most fundamental and inexpensive type of sputtering for PVD metal deposition and electrically conductive target coating materials. If one is doing metal deposition for coating, two major benefits of DC as a source of power for this process is that it is a low cost option and is easy to control. It is used for gold sputter coatings of jewellery, watches and other decorative finishes, for non-reflective coatings on glass and optical components, as well as for metalized packaging plastics. The basic configuration of a DC Sputtering (equipment as shown in **Figure 2.2**) coating system is the target material to be used as a coating is placed in a vacuum chamber parallel to the substrate to be coated. The vacuum chamber is evacuated to a base pressure removing gases and moisture [45].

Figure 2.2: Outlook of DC sputtering machine used.

2.2 Mechanism

Generally, the raw materials used are metal alkoxides for the sol–gel process. But the preparation of a sol is quite tedious and the price of the reagents of the metal alkoxides is quite high. Therefore, many thin films are being prepared with the help of metal salts as the starting materials. In this study, we are making an attempt to obtain a suitable sol from simple salts such as acetates, the reason being, they are more convenient to use as well as less expensive. Usage of acetate salt of the metal was preferred instead of commonly used alkoxide because of its less susceptibility toward moisture.

Several types of solutions have been used as starting solutions for thin film deposition in order to draw conclusions. Here ZnO thin films were grown using a combination of zinc acetate dihydrate ($Zn(CH_3COO)_2 \cdot 2H_2O$) as a zinc precursor and 2-methoxyethanol($C_3H_8O_2$) as a source of hydroxyl groups. Monoethanolamine was used as sol stabiliser. The molar ratio of MEA to zinc acetate was 0.5 and concentration of the solution was 0.5*M [46]*. Zinc salt was dissolved in 2-methoxyethanol by stirring at 60°C. MEA was then added to this solution as it helps to yield a clear and homogeneous solution. It was stirred for 1 hour at 60°C. The solution was left to age under room temperature for different periods of time as in 1day, 2days, 20days, 40days and 60days.

The equation of the reaction is -

$$Zn(CH_3COO)_2.2H_2O + MEA \rightarrow [Zn(MEA)]^{2+} + 2CH_3COO^-$$

$$[Zn(MEA)]^{2+} \rightarrow Zn^{2+} + MEA$$

$$2(OCH_3)C_2H_4OH \rightarrow 2(OCH_3)C_2H_4^{+} + 2OH$$

$$Zn^{2+} + 2OH^- \rightarrow Zn(OH)_2 \downarrow$$

$$Zn(OH)_2 \rightarrow ZnO + H_2O \uparrow$$

(↑ tells evaporation and ↓ tells precipitation)

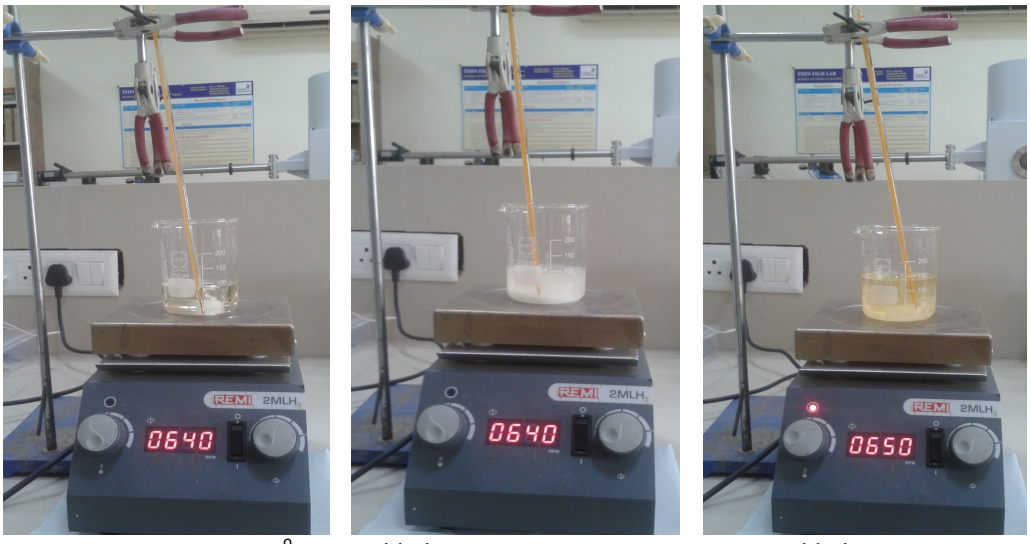

2-methoxyethanol at 60 °C | Added Zinc acetate dehydrate | MEA added

Figure 2.3: Photographs of growth of solution required for the spin coating process.

Above **figure 2.3** illustrates that when to 2-Methoxyethanol, Zinc salt was added at 60°C with constant stirring, the solution turns white as the salt is dispersed in it. To this, when MEA was added, solution turned pale yellow and the dispersed salt particles began to mix with the reagents. It turns into clear solution after an hour of stirring.

ZnO thin films were prepared by spin coating the aged solution onto ultrasonically cleaned glass substrate fixed on the rotating stage. The rotation speed of 3000 rpm was set for a duration of 30 s. We then took sol in a 5 ml dropper and ten drops were laid at the centre of the substrate while it was accelerating. In order to produce films that are free of voids and cracks and also to achieve thickness, more than one layer of coating is usually needed. Numbers of layers were also varied for the optimisation. Variation was in terms of 15, 30, 50 coatings as explained in **figure 2.4** flowchart.

The samples were placed in a furnace for crystallization and in order to remove unwanted volatile material. They were thermally annealed at a rate of 5°C/min from room temperature

to a final temperature of 520°C. Samples were maintained at this temperature for 1 h before being air-cooled to room temperature.

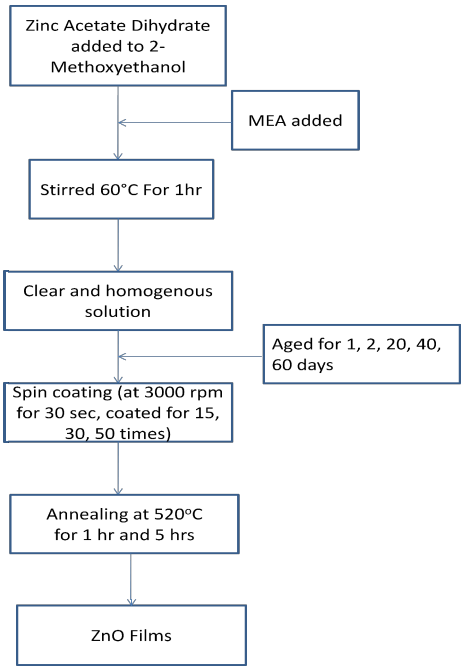

Figure 2.4 Flowchart of the solution process and the spin coating method employed.

The thicknesses of the deposited thin films depend on a number of factors, namely, spin speed, spin duration and solution viscosity. The last factor is in turn determined by solution concentration and evaporation rate of the base solution.

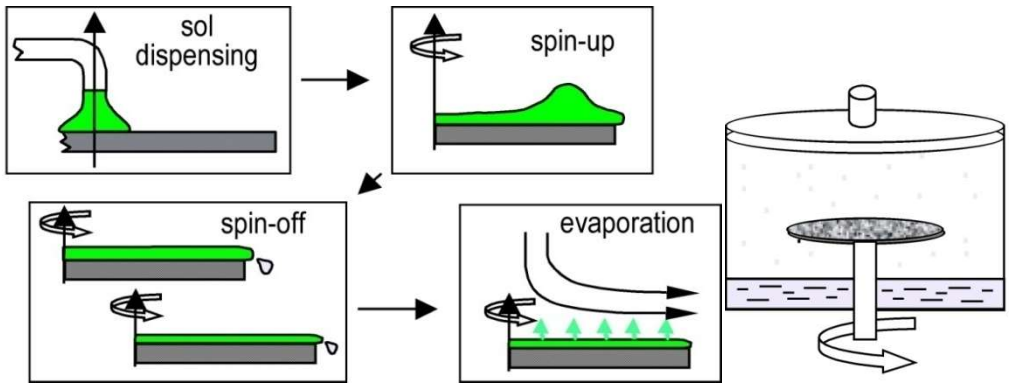

Figure 2.5: Schematic of working criteria of spin coating method.

Above **figure 2.5** depicts the mechanism involves in spin coating a film onto a substrate. The drops of the solution are dispensed on the rotating substrate. This rotation causes the solution to spread over the substrate uniformly and spins off the rest of the solution.

For deposition of second layer comprising of Gold, DC sputtering via auto fine coater system was used. ZnO coated glass slides were placed on the sample stage and vacuum of 4Pa was attained. Current of 30mA was set and the sputtering was turned on for different time intervals as in 1 min, 2 min and 3 min in order to have different thicknesses of 3nm, 6nm and 9nm respectively [47]. Pink plasma was observed. For agglomeration of the gold layer, these were annealed at 400^{o}C for different intervals of 2hrs, 4hrs and 6hrs.

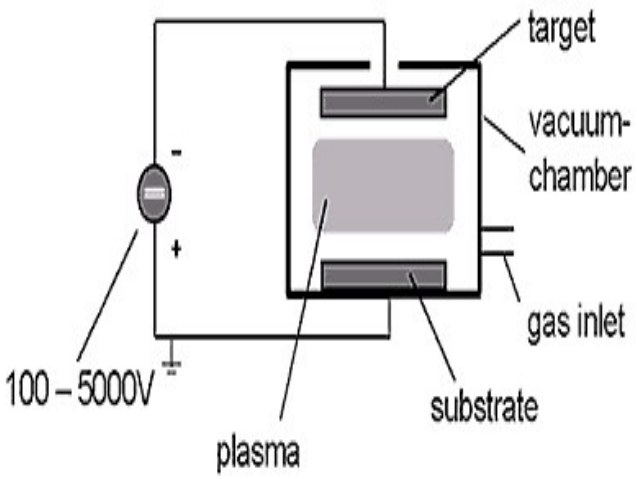

Figure 2.6: Schematic of DC sputtering system.

Above **figure 2.6** shows the arrangement used for DC-sputtering where substrate and target opposes each other in the vacuum chamber separated few centimeters. The substrate and chamber walls act as the anode whereas the target acts as cathode because it is connected to the negative output of a DC power supply.

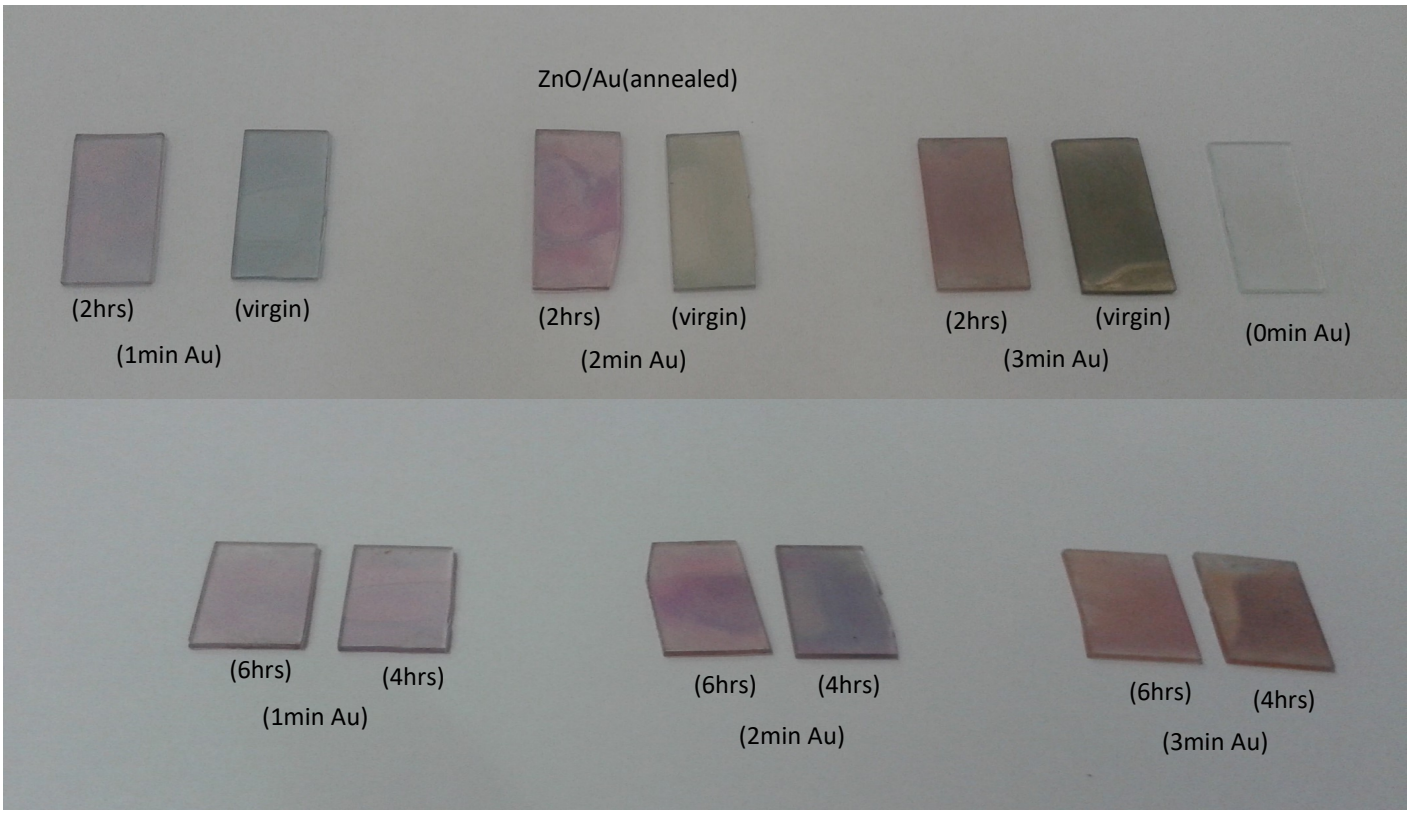

Figure 2.7: Glances of the sample with bottom layer of ZnO and the above layer of Au. Top row with as deposited and 2hrs annealed Au. Bottom row with 2+4hrs and 4hrs annealed Au.

This **figure 2.7** has the samples of spin coated ZnO film and sputtered Au layer with varying thickness. Colour of as deposited samples vary from grey to brown. Grey depicting lesser concentration of Au and brown showing maximum amount of Au deposited. Wherein, ZnO sample is white in appearance. When these are annealed at 400^{o}C for different durations, colour seemed to change accordingly. Small amount of Au turns pink on annealing while sample with larger content of gold turns orange.

Finally, the capping ZnO layer that is the third layer was spin coated the same way as mentioned above.

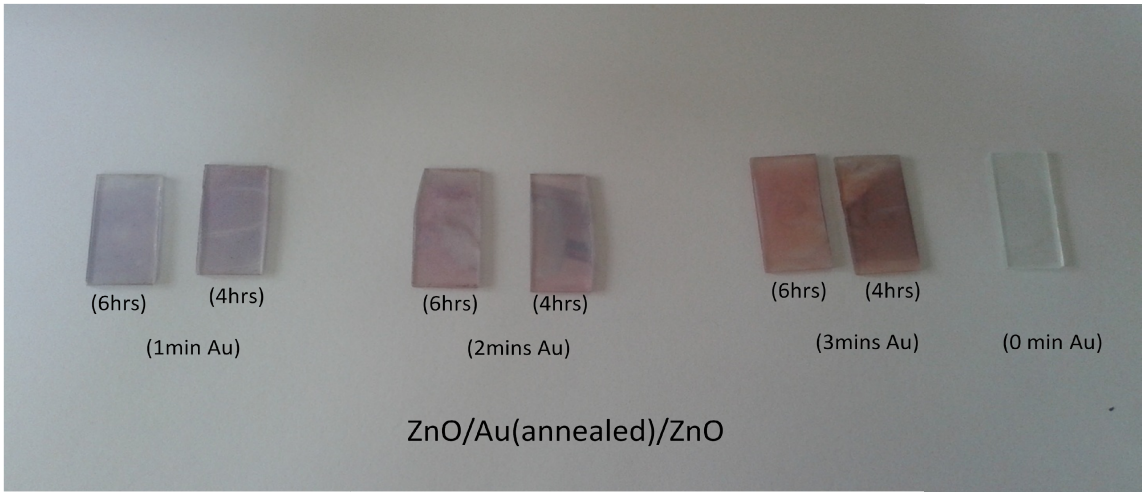

Figure 2.8: Photograph of final samples of the tri-layered films with mid layer Au annealed at 2+4hrs and 4hrs.

Final ZnO layer in the sandwich structure lighten the colour of the previously obtained samples as presented in **figure 2.8**.

The resultant sandwich structure is obtained as in **figure 2.9**. Annealing causes film to change from inside out. To study the change some characterizations are performed, which are given in next section.

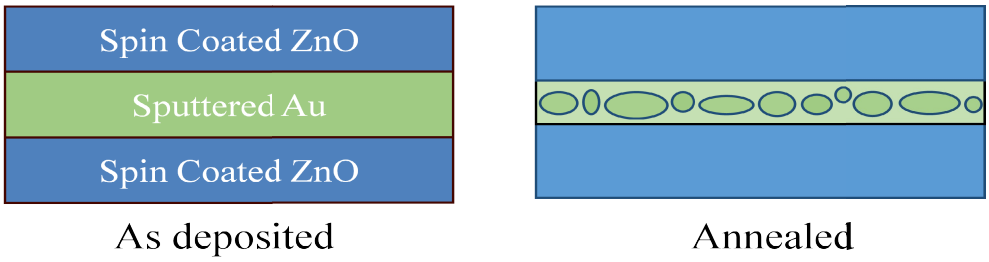

Figure 2.9: Schematic of film so formed.

2.3 Characterisation Techniques

2.3.1 TGA/DSC

Thermogavimetric analysis (TGA) measures the rate and the amount of weight changes of a material with respect to time or temperature in a controlled environment as portrayed in **figure 2.10**. TGA consists of three major parts: a furnace, microgram balance and a

thermocouple. Microbalance helps in monitoring weight of the sample as a function of temperature. The sample hangs from the balance inside a furnace and is itself thermally isolated from furnace.

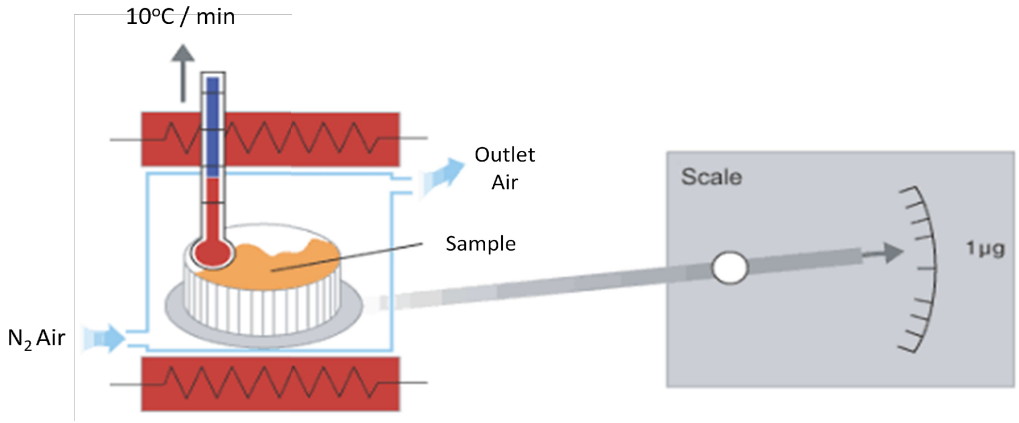

Figure 2.10: Schematic of internal view of TGA measurement.

It is an analytical technique for measurement of the changes in the mass of a material that happens in response to programmed changes in temperature. These changes can be caused by a variety of processes as in vaporization, decomposition, sublimation, degradation, adsorption, desorption, reduction, and oxidation [48].

Differential Scanning Calorimetry (DSC) measures the flow of heat and temperature associated with transitions in sample as a function of temperature and time in a controlled environment. This provides qualitative and quantitative information about alterations in physical and chemical properties that involves changes in heat capacity or exothermic or endothermic processes [48].

DSC apparatus is built with data acquisition device, temperature controller, signal amplifier, differential detector, furnace and a gas control device as shown in **figure 2.11** below.

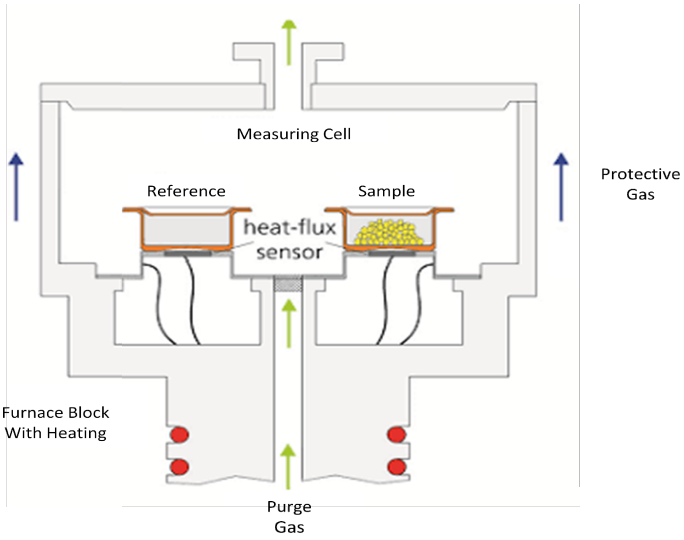

Figure 2.11: Schematic of internal working of DSC measurement.

The main application of DSC is in studying the transitions of the phase, such as glass transitions, or exothermic, endothermic decompositions or melting. These transitions engage heat capacity changes or energy changes that can be detected with great sensitivity by DSC. Instrument outlook used for this analysis is as shown in **figure 2.12**.

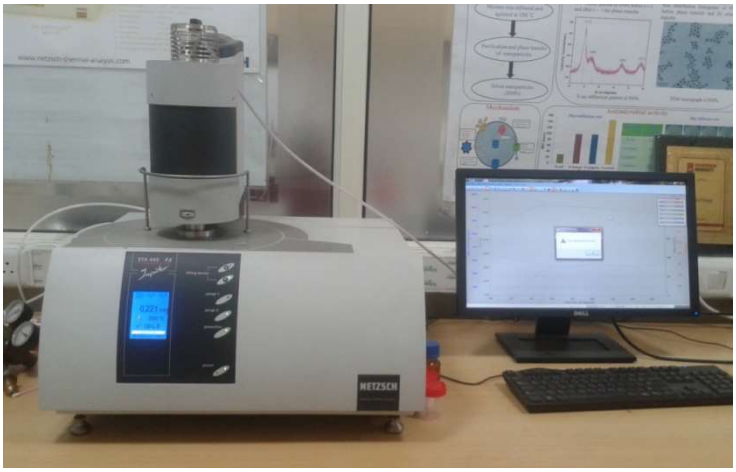

Figure 2.12 TGA/DSC equipment used.

2.3.2 X ray Diffraction (XRD)

XRD is a non destructive practice for determining the chemical composition, physical property and crystal structure (crystalline or amorphous) of the material. It gives knowledge on phase, preferred crystal orientation and other parameters of structure like crystallinity,

average grain size, strain as well as crystal defects. XRD peaks are formed by constructive interference of monochromatic x-ray beam which is to be diffracted at definite angles from each lattice planes set in a sample. By changing the angle of incidence of the beam continuously, a spectrum of obtained diffraction intensity versus angle between incident and diffraction beam is noted. Therefore, in any given material, as far as analysis of periodic atomic arrangements is concerned, the X-ray diffraction pattern is like the fingerprint for such study**.** A search of the ICDD (International Centre for Diffraction Data) database of patterns of XRD helps to identify the phase of variety of samples being crystalline [48].

Main components of diffractometer are:

- Source of X-Ray- X-Ray Tube
- Conditioning the X-Ray beam before it strikes the sample- Incident beam optics
- Platform that holds and moves the detector and tube- Goniometer
- To condition the X-Ray beam after it has encountered the sample- Receiving side optics
- Sample holder
- To count number of X-rays scattered by sample / detector.

It works on Bragg's law as illustrated in **figure 2.13**. This law related the wavelength of electromagnetic radiation to the angle of diffraction and the lattice spacing in the sample. Detection, processing and counting is then done of diffracted X-rays. θ is the angle between source of X-ray and the sample whereas 2θ is the angle formed between detector and incident beam.

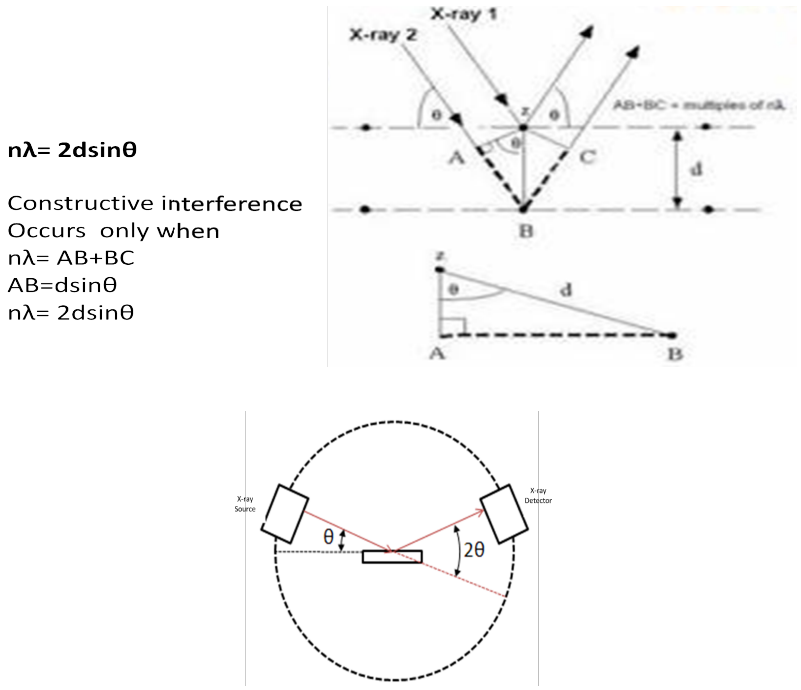

Figure 2.13: Principle of Bragg's law.

The detector records and processes the output signal of X-ray and converts it in a count rate which is then output to a printer or a monitor device. By examining the sample through a range of 2θ angles, all possible directions of diffraction of the rays from the lattice would be attained due to orientation of the sample.

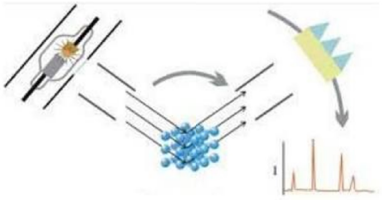

Different planes in a crystal give different signals = positive interference of waves

Figure 2.14: Showing the overall idea of working of XRD on the left and the XRD system used on the right.

XRD equipment is as shown in **figure 2.14** and the overall mechanism of giving pattern is also drawn with it.

2.3.3 UV-VIS SPECTROSCOPY

Ultraviolet and visible (UV-Vis) spectroscopy gives the measurement of the attenuation of light beam passing through the sample or reflecting from sample surface. Measurement of absorption can be over an extended spectral range or at a single wavelength. The absorption spectra arises from transition of electron from lower level to higher level [48].

Parts of this spectrometer are:

- Light source (Tungsten filament and hydrogen deuterium are mostly used)
- Monochromator (Composed of prisms and slits)
- Sample and reference cell
- Detector (photo cells are used)
- Amplifier (Coupled with servometer)

Outlook of the equipment is shown in **figure 2.16**. The setup is attached with computer monitor as the recording device.

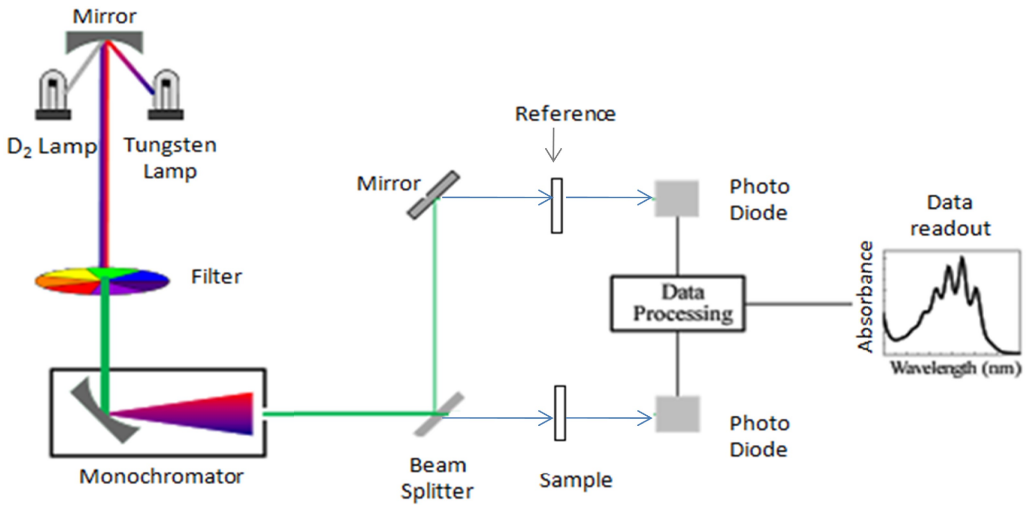

Figure 2.15: Schematic of internal working of UV-VIS Spectrometer.

Figure 2.15 demonstrates that light from tungsten falls on monochromator, which through beam splitter goes half towards sample and half towards reference sample. Transmittance, reflectance and absorption are received on basis of nature of sample. It works on the principle of Beer-Lambert Law, which says that intensity of light changing after passing through a sample should be proportional to path length, concentration of sample and intensity of incident light. It provides quantitative measurement of analyte and optical and electrical properties of a material. UV-Vis includes transmittance, absorption and reflection measurement in UV-Visible and near Infrared regions where absorption is related to transmittance as A= -log(%T).

Figure 2.16: Outlook of the UV-Vis spectrometer used.

2.3.4 SEM

A scanning electron microscope (SEM) is a type of electron microscope that scans the sample surface in araster pattern with the help of a high energy electron beam. This focussed beam of electrons scans the surface of the sample and produces its image. Instrument is shown as **figure 2.18** The interaction of electrons with the atoms of the sample and produce a number of signals that contains information about the topography, composition, morphology and other properties such as electrical conductivity [48].

SEM chamber consists of two detectors that are used to detect the two types of electrons that are coming back from the gold metal specimen. It is these electrons called as secondary and backscatter that go to build up an image of the specimen. This image of the electrons is what

we see and not the image formed by reflected light as we see in a light microscope. Its internal peek is given in **figure 2.17**. The gold sputter coater is a machine that is employed to coat the prepared specimens in gold before they are tested for SEM. The reason why we gold coat the specimens in order to make the sample conductive and also because the SEM doesnt use light globe, instead an electron beam is used to illuminate the specimen. If the sample is not finely coated with a metal like gold, a very poor or weak signal is received and thus the image formed will be very dark and possibly may not even be there. More of a specimen can be in focus at one time as SEM has a large depth of field. Its resolution is high enough that even closely spaced samples can be magnified.

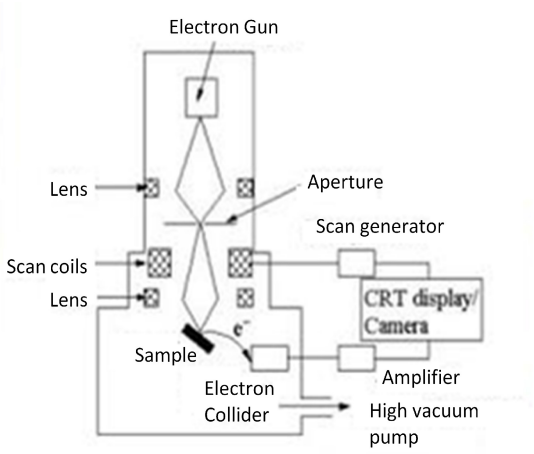

Figure 2.17: Schematic of internal working of the SEM system.

In SEM, there is electron gun fitted with tungsten filament cathode that thermionically emits an electron beam. Tungsten is normally used because of its high melting point and low vapour pressure. Energy of electron beam ranges from few hundred eV to forty keV is produced by electron gun at the top of microscope. Beam of electron follows vertical path through the microscope within a vacuum. In the electron column, this beam passes through pair of plates of deflector (typically in the final lens) which deflect the beam in both axes- X and Y. This is so that it scans in a raster manner over the surface of sample. Once the sample is hit by the beam, electrons and X-rays are ejected from it. Detector collects this back scattered electrons, X-rays and secondary electrons and convert them into final image.

Figure 2.18: Picture of SEM instrument used.

CHAPTER 3

EXPERIMENTAL RESULTS AND DISCUSSION

In this chapter, the results of various investigations carried out on the samples have been presented and discussed in detail.

3.1 TGA/DSC STUDIES

To analyse the influence of the annealing temperature and weight change of the precursor, reagents and precursor solution, DSC and TGA were carried out using STA 449 F3 Jupiter, NETZSCH Geratebau GmbH.

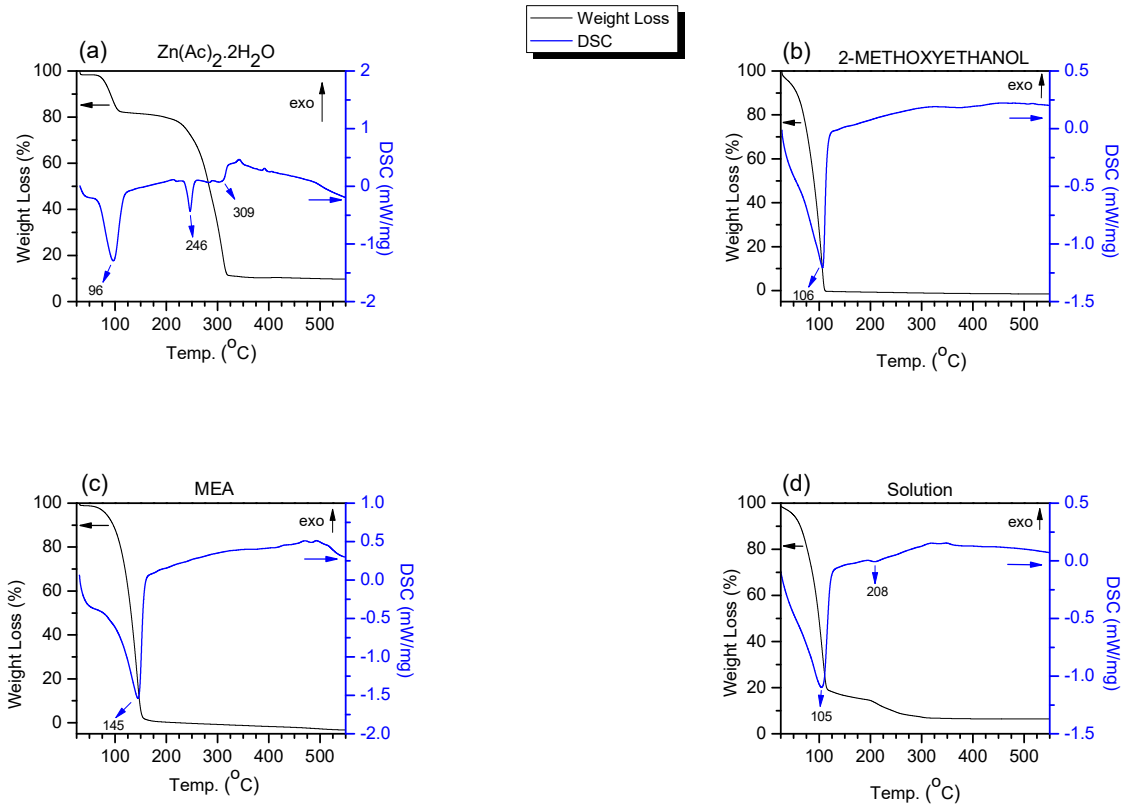

Figure 3.1 Showing typical TGA/DSC curves of the chemicals used for preparing the ZnO thin films via the spin coating technique.

Figure 3.1(a) depicts that when heated in air, Zinc Acetate Dihydrate ($Zn(OAc)_2$) develops three endothermic peaks in DSC at 96°C, 249°C and 309°C. It starts to dehydrate around 100°C and become anhydrous. Further decomposition between 150°C to 280°C shows formation of $Zn_4O(CH_3CO_2)_6$ which finally forms ZnO. Thus the thermal decomposition finishes at 310°C. Wherein TGA shows significant weight loss in 95-110°C and 215-315°C. The latter interval involves major loss in weight.

Figure 3.1(b) illustrates 2-Methoxyethanol having a significant weight loss in 0-100°C due to material evaporation and stays steady after that till 550°C. Its DSC curve shows an endothermic peak around 106°C pointing decomposition. It has boiling point near 125°C and is most preferred hydroxyl group due to high boiling point.

Figure 3.1(c) presents MEA's reaction to increasing temperature. TGA shows that loss in weight happens in 0-150°C and continues to be almost constant after that. It has a boiling point of 170°C happening within interval of 69°C-70°C. Also DSC graph gives an endothermic peak at 145°C showing decomposition. It works as complexing agent which retards condensation of Zn^{2+} thus helping formation of ZnO.

High boiling point solvents are used as they help in forming aligned grain growth and thus helps in strong preferential orientation of crystals. They allow structural relaxation before crystallisation because they evaporate slowly on being heated. Whereas ones with low boiling disturb the alignment as they inculcate stress in structure.

Figure 3.1(d) depicts TGA of Solution of all the above reagents undergoing weight loss. It is mainly in interval 0-110°C. After 110°C it shows gradual decrease till 250 °C and becomes steady after that. This is due to combustion of organics such as ethoxy group and evaporation of water. DSC curve shows majorly two endothermic peaks. First at 105°C indicating evaporation of water and second at 208°C conveying evaporation of 2-methoxyethanol and decomposition of residual organics and MEA.

Above 500°C, there is no significant heat flow change or loss in weight, thus summing up to a conclusion that 500°C would be most suitable temperature for decomposition and consequencing in ZnO.

3.2 XRD Studies

XRD patterns were carried out using PANalytical's X'pert PRO for various durations of first stage annealing temperatures, for different ageing periods for ZnO and thus optimising it for the sandwich structure with gold layer in the middle.

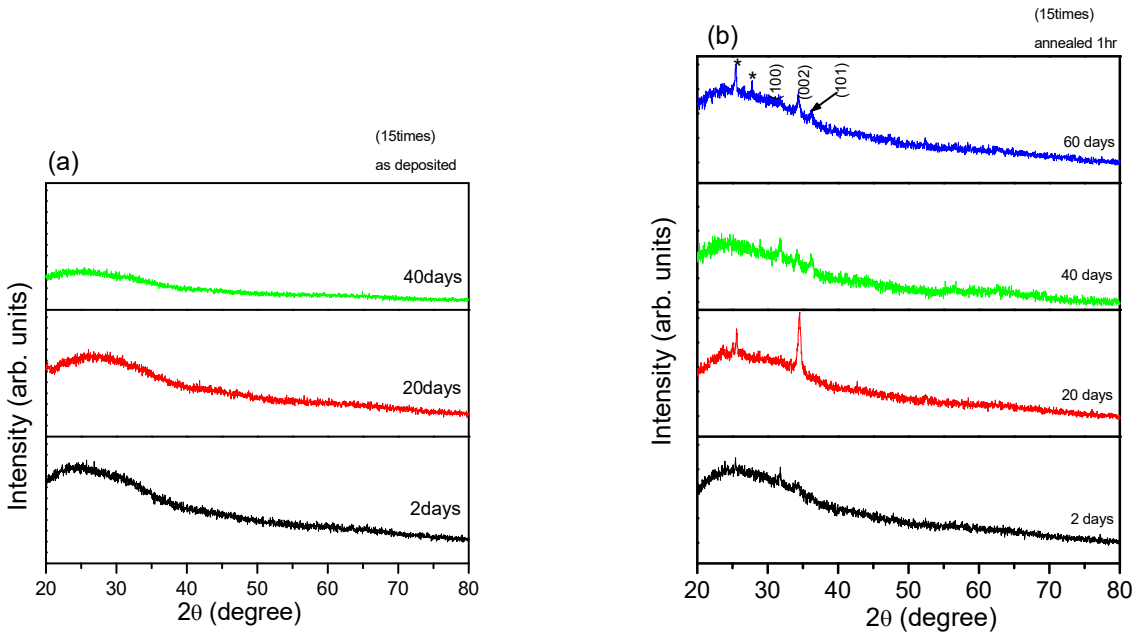

Figure 3.2 XRD patterns showing the effect of ageing on (a) virgin and (b) annealed samples of ZnO thin films.

Figure 3.2(a) shows typical XRD patterns of the as deposited ZnO thin films aged for different durations and grown at room temperature with each film consisting of 15 layers, as described in chapter 2. The patterns are featureless except for a broad hump around 20-30^{o} corresponding to the diffraction from the amorphous glass substrate.

However, **figure 3.2(b)** shows that annealing of the films at 520^{o}C for 1hr resulted in partial crystallization of the films, as characterized by peaks of small intensities corresponding to wurtzite ZnO phase (JCPDS data card: 00-036-1451). Pattern displayed mainly three peaks corresponding to (100), (002) and (101). It may be noted that there were some sharp peaks marked by asterix (*) in the patterns that could not be identified with the compounds used or metallic Zn or ZnO. It might have originated from the sample holder used in the XRD measurement.

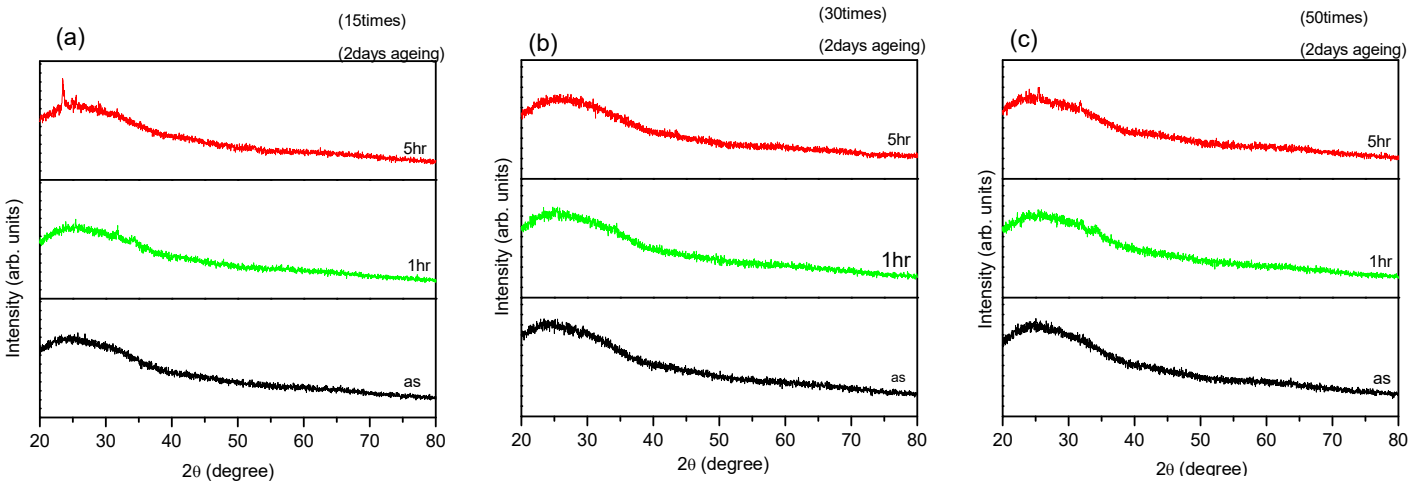

Figure 3.3 Illustrating effect of annealing duration on samples coated with (a) 15 layers, (b) 30 layers and (c) 50 layers.

In order to determine the effects of annealing the thin films, the film grown from the solution aged for 2 days was used. The number of layers was varied from 15 to 50 and the annealing duration was varied from 1hr to 5hrs.

However, as the **figure 3.3(a), (b), (c)** reveal, there is not much change in the XRD patterns of the films so made. It suggests that for a given ageing period of the solution, annealing duration and the number of coatings in the film did not influence the crystal structure of the resultant film.

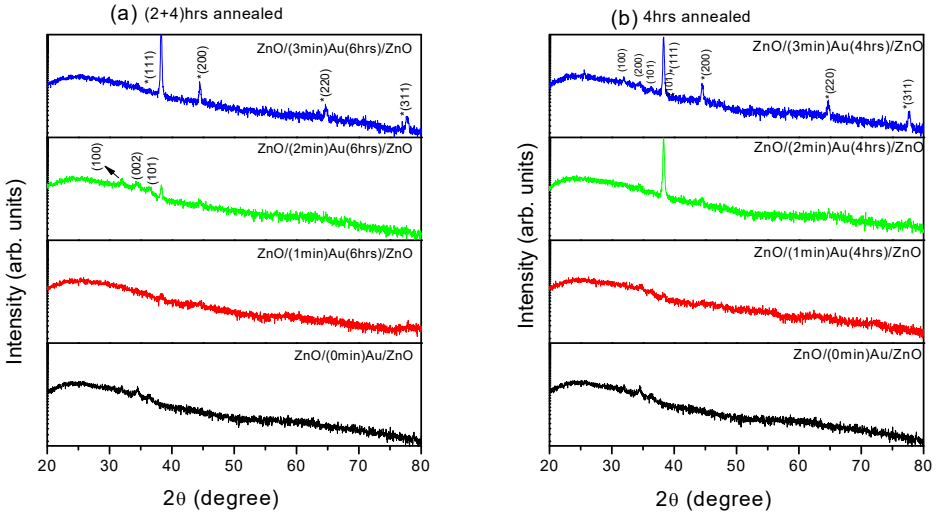

Figure 3.4 Depicting the effect of concentration of Au in sandwich structure when Au was annealed for different periods as in (a) 6hrs and (b) 4hrs.

Figure 3.4(a) shows XRD patterns for sandwiched Au structure annealed at 2hrs first and then for another 4hrs making it discontinuous 6hrs duration. When concentration of gold is varied from 0min to 3min, XRD pattern shows growing peak intensity at $2\theta = 38^0$, 44^0, 64^0 and 77^0 indicating planes (111), (200), (220) and (311) respectively for Au (JCPDS data card: 03-065-2870). Thus proving that samples have polycrystalline structure of Au. The top layer of ZnO shows 31^0, 34^0 and 36^0 prominent peaks, also ZnO/ZnO exhibit hexagonal structure.

Figure 3.4(b) displays similar case as above but the middle Au layer is annealed for 4hrs straight. Their concentration has been varied though. Au shows sharp Bragg's peaks at 38^0, 44^0, 64^0 and 77^0 and ZnO at 31^0, 34^0 and 36^0 corresponding to (100), (200) and (101) planes. Au peaks are seen to be growing as we move up from 0min to 3min.

Thus it can be said that annealing provided thermal energy to atoms to diffuse and stack thus crystal structure is seen. This explains difference in patterns when annealing duration is changed. Hence indexing of these patterns can be as wurtzite phased ZnO and face centred cubic (fcc) Au.

3.3 UV-Visible Spectroscopy Analysis

In thin film sciences, optical properties change significantly, especially when metal nanoparticles are in the picture. Optical absorption, transmission and reflectance spectra were recorded in the wavelength range 100nm -1400 nm using Shimadzu UV-2600. Metal nanoparticles have optical properties crucial about their particle shape and size, composition and the local environment.

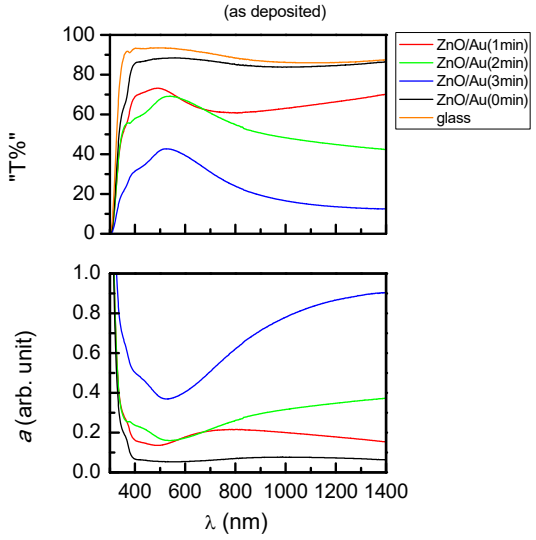

Figure 3.5 Exhibiting effect of concentration of Au in as deposited ZnO/Au film by deposition Au via sputtering method for 0, 1, 2 and 3min.

Above **figure 3.5** has Glass showing 93% transmittance, ZnO showing transmittance of 85-90%. When Au layer is coated on this ZnO, its optical transmittance is deteriorated. Further when concentration is increased, transmittance keeps decreasing and reaches to 30-45% with the maximum concentration of Au when sputtered for 3min. **Figure 3.4** clearly shows the reduction in transmittance and simultaneous rise in absorption. Also these as deposited samples show broad hump showing Au is a continuous film.

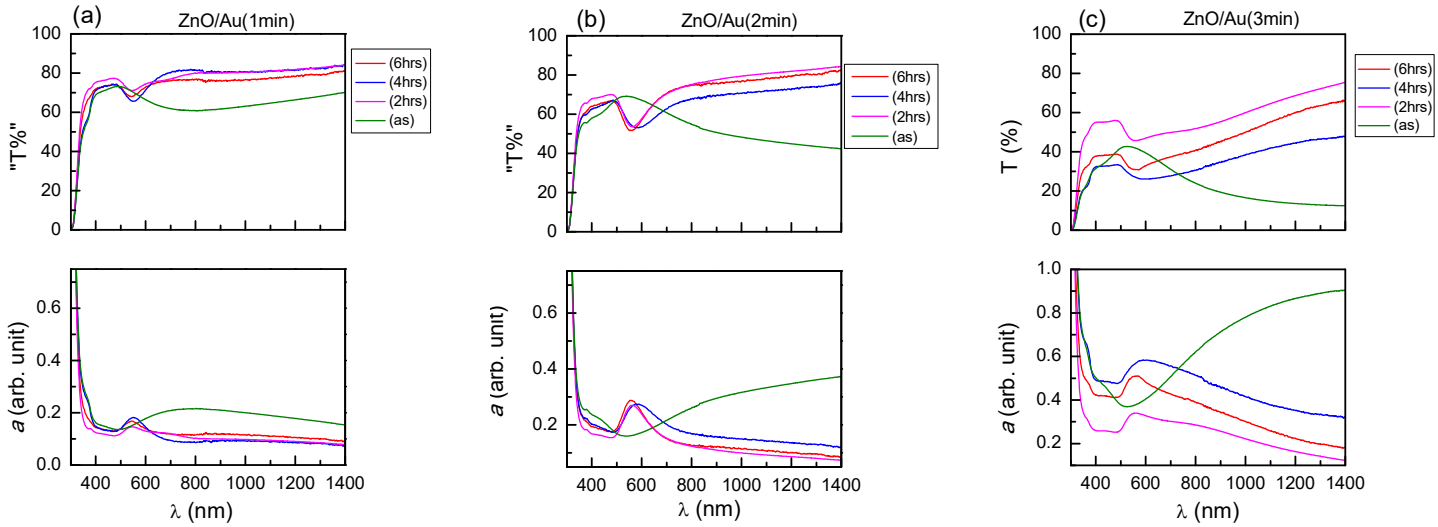

Figure 3.6 Presenting the effect of annealing duration on Au in ZnO/Au when latter layer is sputtered for (a) 1min, (b) 2min and (c) 3min.

Figure 3.6(a) shows that as deposited samples of ZnO/Au shows flat peak in absorbance and has transmittance around 70% and no dip because Au is a continuous layer. Wherein, when it is annealed for 2hrs, 4 hrs and 2+4hrs(6hrs), there is a peak and dip in spectrum which is known as plasmon resonance peak which shows that on annealing, gold has agglomerated or has partially formed gold nanoparticles. The position of plasmonic peak depends on nanoparticle size and shape, metal composition and dielectric properties of the medium of surrounding substrate. But these peaks are broad signifying particles so formed on annealing are not of uniform shape and size. Peak of sample annealed at 4hrs is sharper (at ~65%) than that in 2hrs (at ~ 70%), while annealed at (2+4)hrs has peak in between them (at ~ 68%) indicating discontinuous 6hrs annealing doesn't have same affect as that of continuous ones. Also, noticeable point is that as the concentration of Au is increased, transmission has significantly decreased and corresponding absorption has increased.

Figure 3.6(b) portrays similar fashion of annealed Au films but at reduced transmission in range of 50-55% and increased absorption if compared to **figure 3.6(a)**. The provided thermal energy helped making islands of continuous Au layer. 6hrs i.e. (2+4)hrs sample has peaks lying in between that of 2 and 4hrs. This tells that temperature driven kinetics were interrupted. Sample was cooled to room temperature after 2hrs of annealing, this caused the start of agglomeration of particles. But when it is heated for another 4hrs, these particles of random shape try forming spheres. This is the reason for asymmetry of plasmon peak. The virgin sample also had lessened transmission of about 65%.

Figure 3.6(c) as the maximum concentration of Au. Due to which there are two consequences, first being that transmission is prominently reduced (in range of 30-50%) and corresponding absorption has significantly increased. Second being, the dip in transmittance and peak in absorbance aren't that sharp as they were in first two former cases. This is because the thermal treatment given to them was not enough to agglomerate that amount of gold in 2, 4 or (2+4)6hrs. This leads to non uniform shape and hence this asymmetry causes broad surface plasmon peaks. Though absorbance has increased but full width half maxima (FWHM) value of the peaks has increased too.

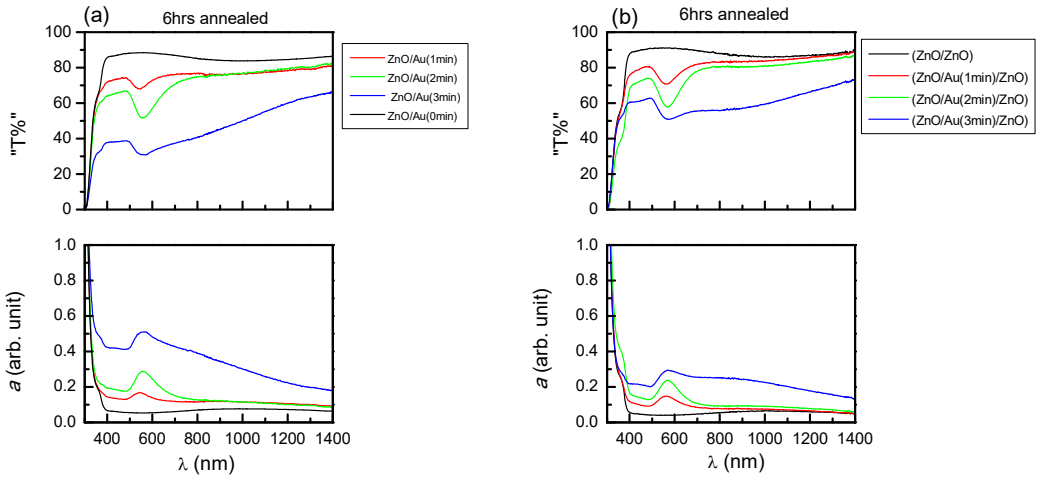

Figure 3.7 Showing the effect of varying concentration of gold in ZnO/Au and ZnO/Au/ZnO films.

In **figure 3.7(a)**, double layer ZnO/Au has been examined with different concentration of gold to see the effect before capping it with third layer.

In **figure 3.7(b)**, sandwich structure with different amount of Au has been analysed. It is observed that peaks undergo a shift towards larger wavelength. Double layer showed absorption peak at 557nm wherein triple layer showed the same at 567nm. This is because the third layer ZnO has affected the plasmon peak.

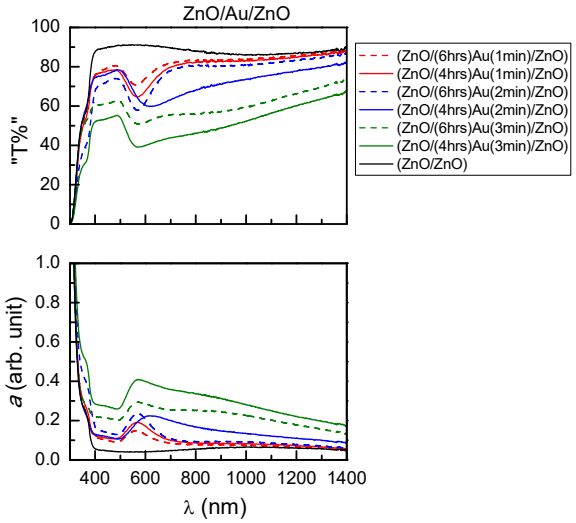

Figure 3.8 Exhibiting the effect of annealing period and concentration of Au in Sandwich structure.

In this above **figure 3.8**, sandwich structures of ZnO/Au/ZnO with varying concentration of Au and varying annealing period have been demonstrated. The absorption at 380 nm takes place due to ZnO, which is characteristic of wide band gap of ZnO. Another absorption band is in range 480–600 nm which is due to the localised surface plasmon peak (LSPR) of the gold NPs. 1min sputtered Au (3nm) shows comparatively sharper peaks. Its 6hr annealed film has lesser absorption than 4hr due to interrupted duration. Its transmittance lies in 65-70%. 2min coated Au (6nm) has little broad absorption peaks and also further 6hrs annealed has greater FWHM value than 4hrs annealed. Its transmittance is around 60%. 3min sputtered Au (9nm) exhibits even broader peaks which may be due to the fact that thermal treatment given was not enough to agglomerate the large amount of gold. Its transmittance is in range 40-50%. Wherein double layer ZnO with no gold content shows 90% transmittance.

It is believed that Au sandwiched layer in ZnO/ZnO film acts as conductive layer and the ZnO films coated on both sides of this interlayer decrease the reflectance from the surface of Au and upholds high optical transmission in the visible region. On the other hand, diffusion of atoms of Au onto the ZnO films by thermal treatment may decrease the effect of antireflection of the ZnO films due to the higher optical absorption of atoms of Au, resulting in lower optical transmittance than that of the as-deposited films.

Also, when calculated optical band gap, there was a reduction observed. ZnO has 3.3eV band gap but with Au layer on top of it, it showed 3.1eV. This is due to interaction of Au atoms with those of ZnO.

It is seen that the optical properties are influenced by the gold content and thermal treatment, also LSPR absorption by gold NPs and photoluminescence in UV - visible ranges.

3.4 SEM Analysis

To have the magnified view of the thin films made, SEM was conducted using Jeol JSM-6510LV. Also to have a clear perspective of how gold layer affects the surface morphology and how annealing influences the film. The samples were coated with a gold later via sputtering in order to make it conductive in nature.

ZnO/ZnO (a) at 5µm and (b) at 1µm

(a) 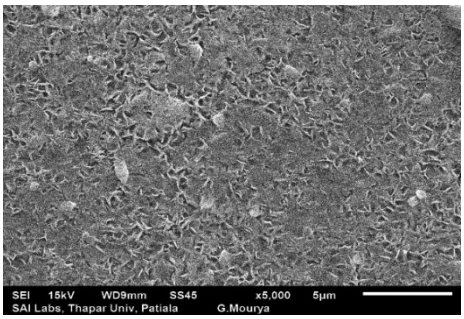

(b) 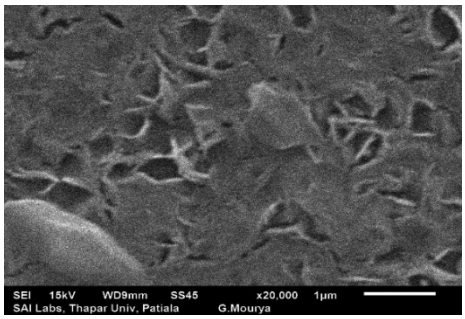

ZnO/Au 1min-4hr/ZnO (c) at 5µm and (d) at 1µm

(c) 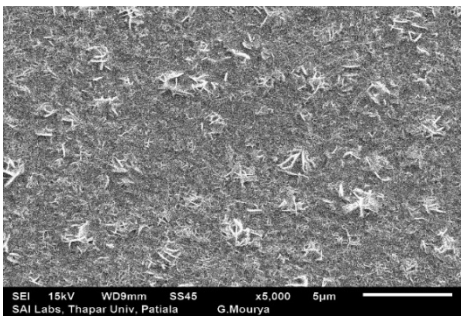

(d) 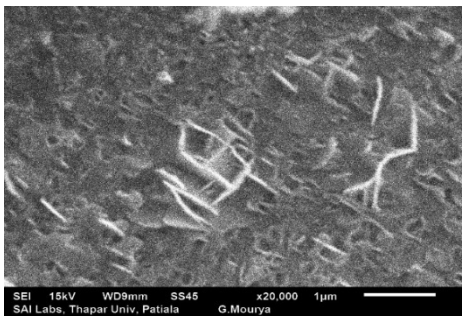

ZnO/Au 2min-4hr/ZnO (e) at 5µm and (f) at 1µm

(e) 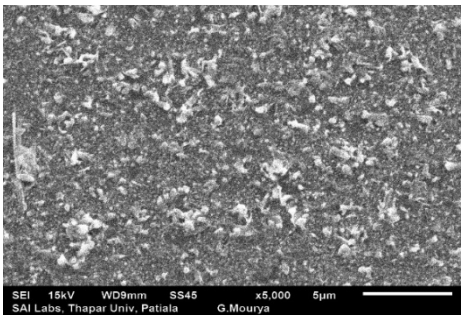

(f) 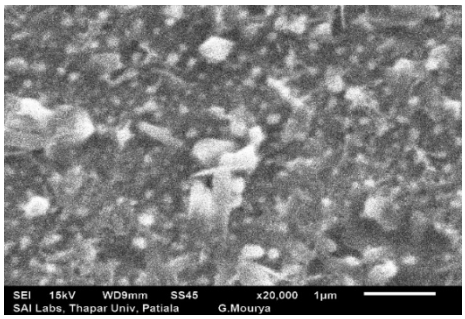

ZnO/Au 3min-4hr/ZnO (g) at 5µm and (h) at 1µm

(g) 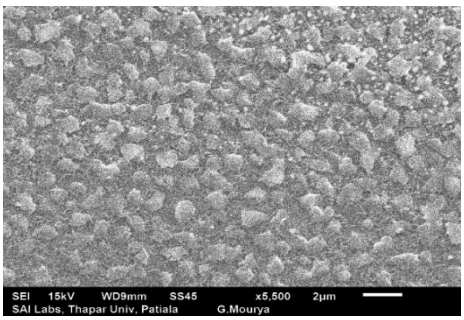

(h) 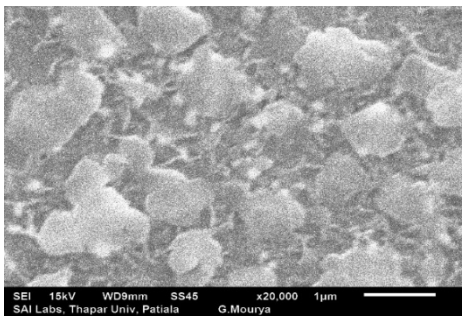

ZnO/Au 3min-6hr/ZnO (i) at 5µm and (j) at 1µm

(i) 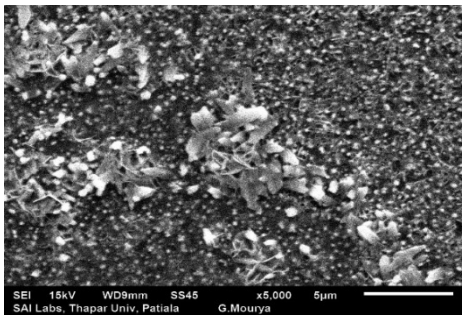

(j) 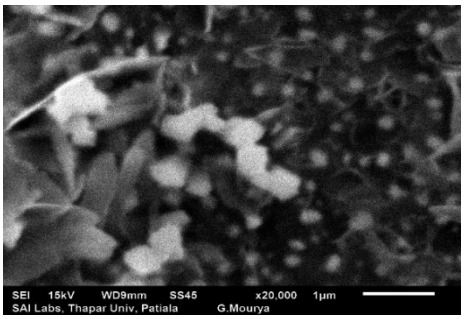

Figure 3.9 SEM images of various SEM samples at two distinct magnification

Figure 3.9 (a) and **(b)** shows images of double ZnO layer. These layers were manually coated using spin coating technique and was annealed at 520^{o}C for 1hr, that is why it results in a rough surface. Annealing does cause stress in the layer which leads to uneven exterior.

Figure 3.9 (c) and **(d)** has Au layer coated for 1 min with possible thickness of 3nm. It was then annealed for 4hrs. as the amount of gold is less, agglomeration of the layer on annealed couldn't be seen on surface with these magnifications.

Figure 3.9 (e) and **(f)** has Au layer coated for 2min and was annealed for 4hrs. Possible thickness of this layer was 6nm. Annealing caused agglomeration and Au particles diffused with the top layer of ZnO thus affecting the surface of the film.

Figure 3.9 (g) and **(h)** encloses Gold layer sputtered for 3 min which was thermally treated for 4hrs at 400^{o}C. Possible thickness of this interlayer was 9nm before annealing. In the image, there are many bright spots dispersed on the background. These bright spots are the aggregated clusters. When zoomed further, they showed island formation of Au layer.

Figure 3.9 (i) and **(j)** has Gold layer with 3 min coating and was annealed for 6hrs at 400^{o}C. Possible thickness of Au layer was 9nm before annealing. After which it has formed particles of non uniform shape and size which are visible on the surface. Annealing causes interaction between layers.

SEM images of **Figure 3.9(a), (b)** is different as compared to the rest as latter have a layer of gold, so this under layer affects the surface morphology of the samples. On the other hand,

comparing images in **Figure 3.9 (g), (h)** and **(i), (j)** samples with same thickness, annealed at same temperature but for different duration shows its affect on the morphology of surface.

Thus, it is a clear evidence that Au changes the surface morphology of the sandwich structured films.

CHAPTER 4

CONCLUSION

The aim of my work was to examine the effect of Au on structural and optical properties of Au NPs embedded ZnO thin films for which ZnO and Au were grown on glass substrate by spin coating process and DC sputtering technique respectively. Zinc acetate dihydate, MEA and 2-Methoxyethanol were used as reagents. All ZnO films were coated at 3000 rpm for 30s. Number of coatings were varied by 15, 30, 50 layers and so was ageing period of the precursor solution was varied by 1, 2, 20, 40, 60 days in order to optimise the growth of the films. Au was coated as second layer on 1 day aged ZnO with 50 coatings. Thickness of Au was varied to see its evolution in the properties. For the sandwich structure, it was then coated with the third layer of ZnO with same conditions. Then the optical properties of the resultant films were characterised by UV-visible Spectroscopy, structural properties by XRD and surface morphology by SEM. Growth of ZnO via solution was analysed by TGA/DSC.

TGA/DSC analysis showed decomposition peaks and boiling points of all the reagents and the solution. It was then concluded that all the heat flow change or loss in weight happens till 500^{o}C. This is why samples were annealed at 520^{o}C to have ZnO films.

Crystalline structure was investigated with XRD studies showed as deposited ZnO under above-mentioned conditions gives amorphous structure wherein annealed ones with different ageing period have peaks showing wurtzite phase of ZnO. Different number of layers and annealing duration were experimented but turns out they didn't affect the film for given ageing period according to XRD patterns. Sandwich structure was tested with varying concentration of Au and different annealing duration. Both the criterion influenced the resultant film which was evident in XRD patterns. Due to thermal treatment, there was interaction in the atoms of the layers. Polycrystalline Au and ZnO structure was observed with Au peaks at 38^{o}, 44^{o}, 64^{o}, 77^{o} and ZnO peaks at 31^{o}, 34^{o} and 36^{o}.

All samples where gold was present showed plasmon peak in UV-Visible spectroscopy which is seen to shift towards higher wavelength when last layer of ZnO is coated. Also, absorption is observed to increase when Au content is increased. Same is the case when samples are

annealed for different duration. It is because of LSPR which is shown due to agglomeration of Au NPs.

SEM analysis reveals the change in surface morphology as the gold content was increased and also as the annealing period was changed. The surface was patchy and rough as annealing causes agglomeration of Au layer which was visible in the SEM images.

All these properties add on to improve the performance of optoelectronic devices.

REFERENCES

[1] N. T. K. Thanh, A. ernhet, Z. Rosenwig " *Springer Ser. Chem. Sens. Biosens*" ***Vol. 3,*** *261,0(2005).*

[2] J. Kobler, B. V. Lotsch, G. A. Ozin, T. Bein, *"ACS Nano"* **Vol. 3**, 1669 (2009).

[3] P. K. Jain, I. H. El-Sayed, M. El-Sayed " *Nanotoday*" **Vol. 2,**18, (2007).

[4] "Synthesis and Characterisation of ZnO Thin film and Nanostructures by Modified Chemical Growth Method For Sensor Applications" by Surya Prakash Ghosh.

[5] "ZnO Transparent Thin Films for Optoelectronics" By Karthik Sivaramakrishnan.

[6] U. Ozgur, V. I. Alivor, C. Lio, A. Teke, M. A. Reshchiaov, S. Dogan, V, Avrutin, S. J. Cho, H. Morkoc "*Journal of Applied Physics*", **Vol. 98**, 041301 (2005).

[7] "Synthesis and Characterisation of ZnO Nanoparticles" By Jayanta Kumar Behera.

[8] N. B. Khelladi N. E. Sari " *Advances in Materials Science*" **Vol. 13**, 35 (2013).

[9] V. A. Coleman, c. Jagdish, DOI: 10.1016/B978-008044722-3/50001-4 (2006).

[10] L. Sagalowicz, G. R. Fox "*Journal of Material Research*" **Vol. 14,** 1876 (1999).

[11] A. I. Ryasnyansaiy, B. Palpant, S. Debrus, U. Pal, A. L. Stepnaov "*Optics Comunications*" **Vol. 273,** 538 (2007).

[12] V. Perumal, U. Hashim, S. C. B. Gopinath, R. Haarindraprasad, W. Liu, P. Poopalan, S. R. Balakrishnan, V. Thivina, A. R. Ruslinda DOI: 10.1371 / Journal.Pone.0144964 (2015).

[13] T. Ning, Y. Zhou, H. Shen, H. Lu, Z. Sun, L. Cao, D. Guan, D. Zhang, G. Yang "*Applied Surface Science*" **Vol. 254,** 1900 (2008).

[14] Z. Jin, L. Gao, Q. Zhou, J. Wang "*Scientific Reports*" **Vol. 5268,** DOI: 10.1038 (2014).

[15] H . Ishiguro, E. Yokoyama, M. Wakaki "*Optical Society of America"* (2012).

[16] "Gold Based Nanoparticles and Thin Films" by Pia Lansaker.

[17] D. N. Jarrett, L. Word "*Journal of Applied Physics*" **Vol. 9**, 1515 (1976).

[18] X. Wang, X. Kong, Y. Yu, H. Zang "*Physical Chemistry C* " **Vol. 111**, 3836 (2007).

[19] T. Tabakova, V. Idakiev, D. Andreeva, I. Mitov "*Applied Catalysis*", **Vol. 202,** 91 (2000).

[20] A. Patra, S. Kasiviswanathan *"International Journal Of Nanoscience"* **Vol. 10,** 601 (2011).

[21] P. S. Huang, D. H. Kim, J. K. Lee *"Applied Physics Letters"* **Vol. 104**, 142102 (2014).

[22] G. Shan, M. Zhong, S. Wang, Y. Li, Y. Liu *"Journal Of Collide And Interface Science"* **Vol. 326,** 392 (2008).

[23] A. Mehrani, D. Dorranian, E. Solati *"J Clust Sci"* **Vol. 26**, 1743 (2015).

[24] E. D. Gaspera, M. Guglielmi, A. Martucci, L. Giancaterini, C. Cantalini *"Sensors and actuators"* **Vol. 164**, 54 (2012).

[25] R. Viter, Z. Balevicius, A. A. Chaaya, I. Baleviciute, S. Tumenas, L. Mikoliunaite, A. Ramanavicius, Z. Gertnere, A. Zalesska, V. Vataman, V. Smyntyna, D. Erts, P. Miele, M. Bechelany *"Journal of Materials Chemistry C"* **Vol. 3,** 6815 (2015).

[26] T. Dixit, M. Shukla, I. A. Palani, V. Singh *"Optical Materials"* **Vol. 62,** 673 (2016).

[27] T. Liu, W. Chen, Y. Hua, X. Liu "*Applied Surface Science*" **Vol. 392,** 616 (2017).

[28] C. Chen, Y. Lu, H. He, K. Wu, Z. Ye "*Applied Physics A*" **Vol. 110,** 47 (2013).

[29] B. Kumari, S. Sharma, V. R. Satsangi, S. Dass, R. Shrivastav "*Applied Electrochem*" **Vol. 45,** 299 (2015).

[30] U. Pal, J. G. Serrano, G. C. Segura, N. Koshizaki, T. Sasaki, S. Terahuchi "*Solar Energy Materials And Solar Cells*" **Vol. 81,** 339 (2004).

[31] F. Stavale, L. Pascua, N. Nilius, H. J. Freund " *The Journal Of Physical Chemistry C* " **Vol. 117,** 10552 (2013).

[32] W. Chamorro, J. Ghanbaja, Y. Battie, A. E. Naciri, F. Soldera, F. Mucklich, D. Horwat " *The Journal Of Physical Chemistry C* " **Vol. 120,** 29405 (2016).

[33] H. Liao, W. Wen, G. K. L. Wong "*Optical Society of America*" **Vol. 23,** 2518 (2006).

[34] N. L. Tarwal, N. S. Harale, P. R. Jadhav, P. S. Patil "*Solid State Physics*" **Vol. 1447,** 393 (2012).

[35] K. Ozga, T. Kawaharamura, A. A. Umar, M. Oyama, K. Nouneh, A. Slezak, S. Fujita, M. Piasecki, A. H. Reshak, I. V. Kityk *"Nanotechnology"* **Vol. 19,** 185709 (2008).

[36] H. M. Lee, Y. J. Lee, I. S. Kim, M. S. Kang, S. B. Heo, Y. S. Kim, D. Kim "*Vacuum*" **Vol. 86,** 1494 (2012).

[37] "Highly Conductive and Transparent ZnO Thin Film using Chemical Spray Pyrolsis Technique" by Vimal Kumar T. V.

[38] D. D. O. Eya, A. J. Ekpunobi, C.E. Okekee "*The Pacific Journalof Science and Technology* " **Vol. 6**, 16 (2005).

[39] M. Smirnov, C. Baban, G. I. Rusu "*Applied Surface Science*" **Vol. 256,** 2405 (2010).

[40] N. Nithya, S. R. Radhakrishnan "*Advances in Applied Science Research*" **Vol. 3 (6),** 4041 (2012).

[41] S. Rezabeigy, M. Behboudnia, N. Nobari "*Procedia Materials Science*" **Vol. 11,** 364 (2015).

[42] A. G. V. Poot, G. R. Gattorno, O. E. S. Dominguez, R. T. P. Diaz, M. E. Pesqueira, G. Oskam "*The Royal Society Of Chemistry*" **Vol. 2,** 2710 (2010).

[43] Z. R. Khan, M. S. Khan, M. Zulfequar, M. S. Khan "*Material Sciences and Applications*" **Vol. 2,** 340 (2011).

[44] "Synthesis and Characterisation of Solution Processed ZnO thin films" by Ahmad Hossein Adl.

[45] "Growth and characterisation of nanostructured Au doped ZnO thin film by RF Co sputtering" by Stefani Davide.

[46] Y. H. Jo, B. C. Mohanty, Y. S. Choo *"Journal of the American Ceramic Society"* **Vol. 92[3],** 665 (2009).

[47] A. Patra, V. D. Das, S. Kasiviswanathan "*Thin Solid Films*" **Vol. 518,** 1399 (2009).

[48] "Instrumental Chemical Analysis: Basic Principles And Techniques" National University of Singapore.